Review

A Roadmap to Exploiting Biocementation for Martian Construction: Pathways, Challenges, and Research Gaps

Shiva Khoshtinat *

Posted Date: 25 June 2025

doi: 10.20944/preprints202506.2121.v1

Keywords: martian construction; in situ resource utilization; biocementation; microbial induced calcium carbonate precipitation; martian environment

 doi:10.20944/preprints202506.2121.v1

Review

A Roadmap to Exploiting Biocementation for Martian Construction: Pathways, Challenges, and Research Gaps

Shiva Khoshtinat

Politecnico di Milano, Department of Chemistry, Materials and Chemical Engineering "Giulio Natta", Milan, Italy; shiva.khoshtinat@polimi.it

Abstract

As ambitions for sustained human presence on Mars accelerate, in-situ resource utilization (ISRU) becomes essential for overcoming the logistical and economic barriers of transporting construction materials from Earth. Biocementation via microbially induced calcium carbonate precipitation (MICP) offers a promising ISRU-compatible alternative, operating under low-energy conditions suitable for Mars' constrained power infrastructure. This review critically assesses the potential of biocementation for Martian construction by examining microbial pathways, Martian regolith chemistry, water availability, and environmental stressors such as radiation, low pressure, and temperature fluctuations. A comparative analysis of Martian regolith simulants and their compatibility with MICP is presented, alongside an evaluation of microbial viability under Martian conditions. Despite growing interest, the literature remains sparse and fragmented, lacking empirical data under relevant Martian analog conditions. This review identifies seven key research gaps and proposes a strategic roadmap to address these challenges. Establishing a rigorous scientific foundation for MICP on Mars will require interdisciplinary studies that integrate synthetic biology, materials science, and planetary engineering to develop viable biocementation systems for extraterrestrial infrastructure.

Keywords: martian construction; in situ resource utilization; biocementation; microbial induced calcium carbonate precipitation; martian environment

1. Introduction

The aspiration to extend human civilization beyond Earth has catalysed unprecedented advancements in space exploration, transforming speculative ideas into structured, multi-agency programs targeting long-term extraterrestrial habitation. Among the celestial bodies within our reach, Mars stands out as the most viable candidate for human colonization due to its relative proximity, geological features, and potential for in-situ resource utilization (ISRU). While the Moon has served as a critical proving ground for robotic and crewed missions, Mars now emerges as the ultimate objective for establishing a sustainable human presence beyond Earth.

Space agencies such as National Aeronautics and Space Administration (NASA), the European Space Agency (ESA), the Russian Federal Space Agency (RFSA), the China National Space Administration (CNSA), and the Indian Space Research Organization (ISRO) have collectively articulated long-term plans for constructing permanent habitats on Mars, envisioning mission timelines as early as the 2040s [1–3]. These initiatives echo earlier lunar exploration efforts, where transport of prefabricated modules and inflatable structures were proposed for establishing bases [1–4]. However, the logistical and financial challenges associated with transporting heavy payloads remain significant, with NASA estimating launch costs of approximately $10,000 per pound to low Earth orbit [5] and $5,000–20,000 per kilogram to the Moon [3]. These costs are expected to escalate significantly for missions to Mars, highlighting the critical importance of ISRU to reduce reliance on

 doi:10.20944/preprints202506.2121.v1

the transport of Earth-based supplies and create a closed-loop system where resources like water, oxygen, and building materials can be recycled or produced locally, ensuring long-term sustainability. This underscores the urgent need for innovative, cost-effective, and sustainable construction strategies that leverage locally available Martian resources.

The Martian regolith, composed primarily of silicates, oxides, and perchlorates, presents a promising medium for ISRU-based construction. Traditional terrestrial methods, such as microwave-based sintering [6] of regolith or sulphur-based concrete [1], face significant limitations for application on Mars due to the planet's constrained energy infrastructure, which will predominantly depend on solar panels or compact nuclear reactors. These techniques are typically energy-intensive and may not be compatible with the limited power availability in Martian habitats. Furthermore, the requirement for infrastructure that is pressurized, resistant to radiation, and thermally stable necessitates the use of materials with exceptional structural integrity and environmental resilience.

Compared to Mars, research on lunar construction is more advanced [7–11], primarily due to the Moon's proximity and the availability of returned soil samples from past missions [3]. In contrast, Mars sample return missions remain in progress, with the earliest return anticipated no sooner than the 2030s. As a result, experimental validation of construction technologies tailored to the Martian environment lags behind. Despite the wealth of environmental data provided by spacecraft missions—including orbiters such as Mars Global Surveyor [12], Mars Odyssey [13], Mars Express [14], the Emirates Mars Mission (Hope) [15], and ExoMars Trace Gas Orbiter—along with landers and rovers like Viking [16], Pathfinder [17], Phoenix [18], Curiosity [19], InSight [20], and Perseverance [21,22] (Figure 1), the practical implementation of biocementation on Mars remains speculative.

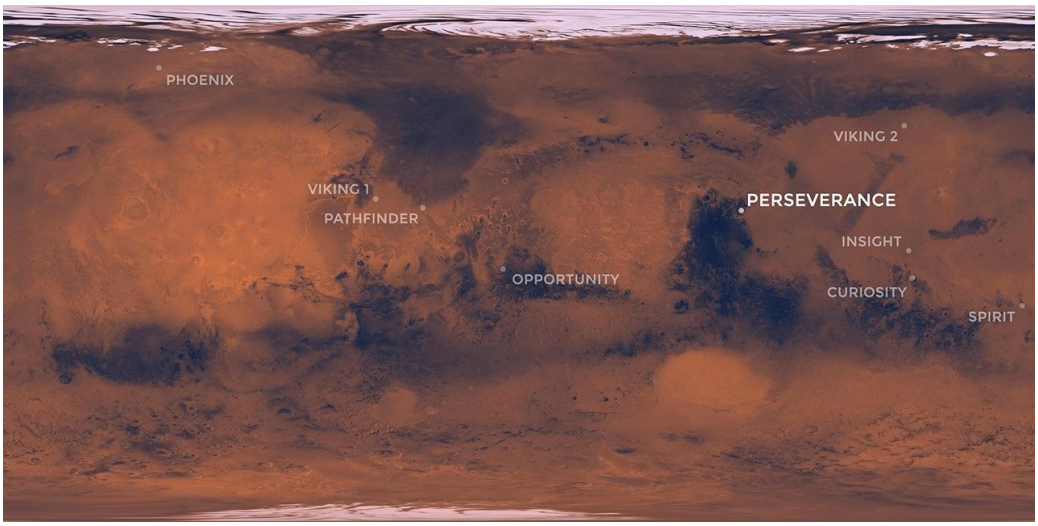

Figure 1. Map of NASA's Mars landing sites, retrieved with permission from [23].

Although some studies have proposed extending extraterrestrial construction methods under investigation for lunar construction, such as sulphur-based concrete, to Mars [24–26], it is important to recognize that the significant differences in environmental conditions between the two celestial bodies can profoundly affect construction techniques, their applicability, and overall performance on Mars. Given that Martian surface conditions, including low pressure, high radiation, perchlorate-rich regolith, and extreme temperature fluctuations, interact in complex ways, a comprehensive assessment of their influence on microbial behaviour and biocementation outcomes is crucial.

In this context, biomineralisation may offer a transformative approach for extraterrestrial construction. This naturally occurring phenomenon refers to the process by which microorganisms induce the formation of minerals under mild, energy-efficient conditions . The process typically initiates when microorganisms attach to a surface that supplies the necessary ions for mineral precipitation [27]. A crucial factor in these microorganism–mineral interactions is the production of

 doi:10.20944/preprints202506.2121.v1

extracellular polymeric substances (EPS), a complex mixture of polysaccharides, proteins, and sometimes DNA, that facilitates microbial adhesion to surfaces [28]. EPS also plays a role in ion accumulation, helping to establish localized microenvironments that promote mineral nucleation by influencing parameters such as pH, redox potential, and ion concentration [27]. Nucleation occurs when ions coalesce into a stable crystalline nucleus on a substrate. Subsequent crystal growth is biologically mediated, with organic molecules often modulating the process by binding selectively to crystal faces and directing shape and structure [28]. The process culminates in the maturation of the mineral product, which may include structural transformations such as the transition from amorphous to crystalline forms.

Martian regolith, which is primarily composed of silicates, iron and aluminum oxides, and perchlorates, presents a promising substrate for microbial biomineralisation. Certain microbial metabolic processes can interact with these mineral components to induce mineral precipitation, thereby enabling the utilization of local resources in accordance with ISRU strategies for Mars. Based on the author's previous investigations, among the various biomineralisation pathways, Microbially Induced Calcium Carbonate Precipitation (MICP), commonly known as biocementation, emerges as the most promising approach for extraterrestrial construction on Mars, owing to its potential for ISRU, structural integrity, and environmental compatibility [29]. Biocementation has demonstrated significant potential in diverse Earth-based applications, including soil stabilization [30–40], building construction [41–51], and wind-induced desertification [52–55] in Earth applications. Its adaptation to Martian regolith could address key challenges such as binder scarcity and in-situ fabrication while aligning with the broader goals of ISRU. Furthermore, in contrast to solar or microwave-based sintering of regolith, biocementation functions at low temperatures with minimal energy requirements, rendering it appropriate for Mars' constrained power systems dependent on solar or nuclear energy.

Although numerous Earth-based studies have demonstrated the potential of MICP as a sustainable construction technology [40–42,51,56–59], only a limited number of publications have explored their viability for extraterrestrial applications [60–63]. The significant disparity in the volume of literature on biocementation for construction on Earth versus Mars stems primarily from the fact that biocementation itself has only attracted substantial scientific attention in the past two decades. Moreover, its application in extraterrestrial environments is a relatively nascent area of research that remains largely unexplored and insufficiently discussed in the current literature. To advance MICP as a viable strategy for Martian infrastructure, empirical studies that rigorously simulate Martian environmental conditions and evaluate microbial activity, survivability, and bio-cementation efficacy are urgently required. However, meaningful progress in this direction depends on a more comprehensive understanding of the Martian environment stressors and their collective impact on the MICP process.

Therefore, this review investigates the potential of biocementation as a viable construction methodology for Mars, focusing on the planet’s unique geological and environmental conditions. Various biocementation pathways including ureolysis, amino acid ammonification, denitrification, sulphate reduction, methanogenesis, and photosynthetic coupling are systematically evaluated with respect to their underlying biological mechanisms and resource requirements. The chemical composition of Martian regolith is critically evaluated as a potential substrate for Microbially Induced Calcium Carbonate Precipitation (MICP), in conjunction with a comparative assessment of currently available Martian regolith simulants. This includes an analysis of their bulk oxide composition and particle size distribution, given the absence of physically returned Martian soil samples. Water availability, arguably the most critical parameter for MICP and any form of construction on Mars is assessed in terms of both potential sources and utilization strategies. The review also examines the Martian atmosphere, including reduced gravity, extreme diurnal temperature fluctuations, high radiation levels, and low atmospheric pressure, and evaluates their collective impacts on microbial viability and metabolic activity.

 doi:10.20944/preprints202506.2121.v1

Although a small number of studies have investigated the performance of biocementation using Martian regolith simulants, the existing literature remains sparse and methodologically fragmented. Rather than focusing exclusively on these preliminary efforts, this review emphasizes the most promising biocementation pathways and outlines a strategic roadmap to address the key environmental and operational challenges associated with implementing such systems on Mars. As with any emerging scientific discipline, the systematic identification of research gaps is essential to guide meaningful progress. Accordingly, this review delineates seven core research gaps and proposes future research directions intended to establish a scientifically rigorous foundation for the development of MICP-based construction technologies suitable for the Martian environment.

2. Biocementation Pathways

Martian regolith, which is rich in silicates, iron and aluminum oxides, and clay minerals, represents a promising in-situ resource for extraterrestrial construction. Future research should focus on the potential of microbial metabolic processes to induce the formation of biominerals using these native mineralogical components. In this context, potential biomineralisation strategies include the use of calcium carbonate–precipitating microorganisms, iron-reducing bacteria[64,65], aluminosilicate-based biomineralisation processes [66], and magnesium carbonate–inducing microorganisms [67]. These approaches are not discussed in detail here but are elaborated upon in a separate investigation by the author [29]. However, among the various biomineralisation pathways, calcium carbonate precipitation, commonly referred to as biocementation, emerges as the most promising and extensively studied method to date. In contrast, the other approaches have not advanced as significantly and have relatively limited literature dedicated to them. Therefore, this study focuses on different pathways of Microbially Induced Calcium Carbonate Precipitation (MICP).

In the past twenty years, MICP has gained considerable interest. This process leverages microbial metabolism to improve the strength and durability of concrete and masonry structures [42,58,59]. This naturally occurring process takes place in diverse environments, including marine and freshwater systems, and involves specific microorganisms whose metabolic activities result in the precipitation of calcium carbonate ($CaCO_3$). MICP offers several advantages over conventional Portland cement-based methods. It requires 43–95% less embodied energy due to its ambient-temperature production, and its carbon footprint is 18–49.6% lower [68,69]. Additionally, the low viscosity of the MICP solution enables it to penetrate concrete pores more effectively, enhancing adhesion and durability [70]. Most importantly, the smaller size of bacteria (<10 μm) compared to cement particles (~40 μm) enables MICP to seal finer pores more effectively. This characteristic is particularly crucial for the biocementation of Martian regolith, which consists of extremely fine particles [71]. The parameters influencing biocementation have been discussed in literature in detail [72,73]; therefore, they are not included here for the sake of brevity. The pathways of MICP can be divided into six categories, which will be discussed in detail in this section: ureolysis, ammonification of amino acids, photosynthesis, denitrification, sulphate reduction, and methanogenesis-induced biocementation [51,74–78].

2.1. Ureolysis

Ureolysis, also known as urea hydrolysis, is the most extensively studied pathway for biocementation in the literature, which involves urease-producing bacteria [40,51,79,80]. In this process, the urease enzyme produced by microorganisms catalyses the hydrolysis of one mole of urea, resulting in the production of one mole of ammonia (NH_3) and one mole of carbamate (NH_2COOH).

$$CO(NH_2)_2 + H_2O \xrightarrow{\text{Urease}} NH_3 + NH_2COOH \quad (1)$$

 doi:10.20944/preprints202506.2121.v1

The carbamate then spontaneously hydrolyses in the presence of water, yielding an additional mole of ammonia (NH_3) and one mole of carbonic acid (H_2CO_3).

$$NH_2COOH + 2H_2O \rightarrow NH_3 + H_2CO_3 \quad (2)$$

Carbonic acid (H_2CO_3) is subsequently converted into bicarbonate (HCO_3^-) and a proton (H^+), a reaction facilitated by the enzyme carbonic anhydrase (CA).

$$H_2CO_3 \leftrightarrow HCO_3^- + H^+ \quad (3)$$

The ammonia (NH_3) produced in the first two steps reacts with water to form ammonium ions (NH_4^+) and hydroxide ions (OH^-), leading to an increase in pH around the microbial cells.

$$NH_3 + H_2O \longrightarrow NH_4^+ + OH^-, pH \uparrow \quad (4)$$

The elevated hydroxide concentration, along with the presence of bicarbonate ions, promotes the formation of carbonate ions (CO_3^{2-}).

$$HCO_3^- + OH^- \leftrightarrow CO_3^{2-} + H_2O \quad (5)$$

In the presence of soluble calcium ions (Ca^{2+}), the carbonate ions (CO_3^{2-}) precipitate as calcium carbonate ($CaCO_3$), contributing to the biocementation process.

$$Ca^{2+} + CO_3^{2-} \rightarrow CaCO_3 \downarrow \quad (6)$$

A diverse array of microorganisms, including microalgae [81–83], fungi [84], and even plant-derived urease enzymes (e.g., those extracted from jack beans) [85–88], as well as several bacterial species such as *Sporosarcina pasteurii* [72,89,90], *Bacillus subtilis* [46,90,91], *Bacillus megaterium* [53,92], and *Bacillus cereus* [49,93], have been reported to induce calcium carbonate ($CaCO_3$) precipitation via ureolysis. Among these, the bacterial species *Sporosarcina pasteurii* has been the most extensively studied due to its high urease activity and notable resistance to harsh environmental conditions, including survival at pH levels as high as 13.6 [72].

2.2. Ammonification of Amino Acids

From a biochemical standpoint, this pathway closely parallels ureolysis. In this process, microbial metabolism breaks down amino acids, releasing carbon dioxide and ammonia (Equation (7)). The ammonia subsequently undergoes hydrolysis in the aqueous microenvironment, producing ammonium and hydroxide ions (Equation (4)). The elevated concentration of OH^- increases the local pH, which, in combination with the dissolved CO_2 forming carbonate species, leads to supersaturation with respect to calcium carbonate. This supersaturation promotes the nucleation and precipitation of $CaCO_3$ (Equations (5) and (6)).

$$Amino\ Acids + O_2 \rightarrow NH_3 + CO_2 + H_2O \quad (7)$$

Certain microorganisms, such as *Bacillus subtilis* [43,45,94,95] and *Bacillus megaterium* [96], are well-known for their ureolytic capabilities and possess the ability to participate in biocementation through the ammonification of amino acids. While other microorganisms, such as *Rhodococcus erythropolis* [97], are known to exhibit amino acid oxidase activity, their direct role in biocementation through oxidative deamination remains underexplored in the scientific literature.

2.3. Photosynthesis

Photosynthetic microorganisms, including cyanobacteria [83,98] and microalgae [82,83], which are predominantly found in aquatic environments, have also been shown to facilitate calcium carbonate ($CaCO_3$) precipitation [74]. For instance, cyanobacterial photosynthesis fixes carbon dioxide (Equation (8)).

$$CO_2 + H_2O \xrightarrow{light} CH_2O + O_2 \quad (8)$$

 doi:10.20944/preprints202506.2121.v1

During this process, high photosynthetic activity reduces ambient CO_2 concentrations, thereby shifting the carbonate equilibrium toward the formation of carbonate ions (Equations. (9) and (10)).

$$CO_2 + H_2O \xrightarrow{light} H_2CO_3 \leftrightarrow HCO_3^- + H^+ \leftrightarrow CO_3^{2-} + 2H^+ \quad (9)$$

This shift leads to an increase in alkalinity (Equation (10)), which facilitates $CaCO_3$ precipitation by promoting the removal of H^+ ions produced during the re-equilibration process (Equation (11)).

$$CO_3^{2-} + H_2O \leftrightarrow HCO_3^- + OH^-, pH \uparrow \quad (10)$$

$$Ca^{2+} + CO_3^{2-} \rightarrow CaCO_3 \downarrow \quad (11)$$

2.4. Denitrification

Denitrification, or nitrate reduction, is an anaerobic respiration process in which nitrate (NO_3^-) serves as the terminal electron acceptor in the absence of oxygen [77,78]. Through a stepwise reduction pathway, nitrate is ultimately converted to nitrogen gas (N_2) (Equation (12)).

$$NO_3^- \rightarrow NO_2^- \rightarrow NO \rightarrow N_2O \rightarrow N_2 \quad (12)$$

In the presence of a carbon source such as acetate and under anoxic conditions, microorganisms oxidize organic substrates using nitrate as an electron acceptor, thereby generating energy required for growth and maintenance (Equation (13)).

$$5\,CH_3COO^- + 8\,NO_3^- + 3\,H^+ \rightarrow 10\,CO_2 + 9\,H_2O + 4\,N_2 \quad (13)$$

This process produces carbon dioxide, which equilibrates with water to form carbonate species. Concurrently, microbial metabolism consumes protons and generates bicarbonate, thus increasing the alkalinity (Equation (14)).

$$CO_2 + H_2O \leftrightarrow H_2CO_3 \leftrightarrow HCO_3^- + H^+ \leftrightarrow CO_3^{2-} + 2H^+ \quad (14)$$

The combination of elevated pH and increased bicarbonate concentration promotes calcium carbonate precipitation in the presence of calcium ions (Equation (15)).

$$Ca^{2+} + HCO_3^- + OH^- \rightarrow H_2O + CaCO_3 \downarrow \quad (15)$$

2.5. Sulphate Reduction

Sulphate-reducing bacteria (SRB) are widespread anaerobic prokaryotes exhibiting considerable morphological and phylogenetic diversity [78]. These microorganisms play a pivotal role in the decomposition of organic matter under anoxic conditions and contribute significantly to the sulphur biogeochemical cycle. In environments with high sulphate availability, sulphate reduction becomes the predominant pathway for organic matter mineralisation. In the sulphate reduction pathway, sulphate-reducing bacteria use sulphate (SO_4^{2-}) as an electron acceptor while oxidising organic compounds or hydrogen.

Equations (16)-(19) depict four representative sulphate reduction reactions, involving different low-molecular-weight electron donors: organic carbon compounds (Equations (16)–(18)) and molecular hydrogen (Equation (19)) [74]. Sulphate-reducing bacteria (SRB) are classified based on their capacity to either fully or partially oxidise organic substrates. Specifically, Equations (16) and (17) illustrate complete and incomplete sulphate reduction of lactate, respectively. In the case of partial reduction, only one-third the amount of calcium carbonate is precipitated per mole of lactate compared to complete reduction. Equations (18) and (19) represent the sulphate reduction reactions coupled with the oxidation of ethanol and hydrogen, respectively.

$$2C_3H_5O_3^- + 3SO_4^{2-} + 3Ca^{2+} \rightarrow 3HS^- + 3\,H_2O + H^+ + 3CaCO_3 \downarrow \quad (16)$$

$$2C_3H_5O_3^- + SO_4^{2-} + Ca^{2+} \rightarrow HS^- + H_2O + 2C_2H_3O_2^- + CO_2 + H^+ + CaCO_3 \downarrow \quad (17)$$

 doi:10.20944/preprints202506.2121.v1

$$2C_2H_6O + SO_4^{2-} + 2Ca^{2+} + OH^- \rightarrow 3HS^- + 5H_2O + 2CO_2 + CaCO_3 \downarrow \quad (18)$$

$$6H_2 + SO_4^{2-} + 2Ca^{2+} + 2HCO_3^- \rightarrow HS^- + CH_2O + 5H_2O + CaCO_3 \downarrow \quad (19)$$

2.6. Methanogenesis

In both marine and freshwater sedimentary environments, methane-oxidising microorganisms significantly influence carbon dioxide concentrations under aerobic and anaerobic conditions. Aerobic methane oxidation enhances carbonate dissolution due to increased acidity, while its anaerobic counterpart promotes calcium carbonate precipitation [51]. Methanogenesis can also occur in environments where sulphate reduction is actively taking place. During anaerobic methane oxidation, methane is converted to bicarbonate while sulphate is reduced to hydrogen sulphide (HS^-) (Equation (20)). The system reaches the carbonate equilibrium (Equation (21)). When calcium ions (Ca^{2+}) are present, this process leads to the formation of calcium carbonate and the release of hydrogen sulphide (H_2S) (Equation (22)). Evidence from methane distribution profiles, radiotracer experiments, and stable carbon isotope data suggests that a substantial fraction of methane in marine sediments is oxidised to carbon dioxide via anaerobic pathways [77].

$$CH_4 + SO_4^{2-} \rightarrow HS^- + HCO_3^- + H_2O \quad (20)$$

$$HCO_3^- + H^+ \leftrightarrow CO_3^{2-} + 2H^+ \quad (21)$$

$$HS^- + H^+ + CO_3^{2-} + Ca^{2+} \rightarrow H_2S + CaCO_3 \downarrow \quad (22)$$

Under aerobic conditions, methane oxidation is initiated by its conversion to methanol, catalysed by the enzyme methane monooxygenase in the presence of molecular oxygen (Equation (23)). Within the cell's periplasmic space of methanotrophic bacteria, methanol (serving as both an energy and carbon source) is further oxidised to formaldehyde and subsequently to formate through a series of enzymatic reactions. When formate reaches equilibrium with formic acid, formate dehydrogenase facilitates the oxidation of formic acid to carbon dioxide (Equations (24)-(27)). The resulting CO_2 subsequently forms carbonate ions (similar to Equation (14)), and in the presence of calcium ions, calcium carbonate precipitates around the microbial cells (Equation (28)) [51].

$$CH_4 + O_2 \leftrightarrow CH_3OH + H_2O \quad (23)$$

$$CH_3OH \rightarrow CHOH + H_2 \quad (24)$$

$$CHOH + H_2O \rightarrow HCOO^- + H^+ \quad (25)$$

$$HCOO^- + H_2O \leftrightarrow HCOOH + OH^- \quad (26)$$

$$HCOOH \rightarrow CO_2 + H_2 \quad (27)$$

$$OH^- + H^+ + CO_3^{2-} + Ca^{2+} \rightarrow H_2O + CaCO_3 \downarrow \quad (28)$$

3. Martian Resources and Environment

Within our solar system, Mars is believed to be the most Earth-like planet (Table 1). Its surface is solid and rocky, similar to Earth's. Mars possesses polar ice caps, evidence of ancient rivers, lakes, and subsurface liquid water, as well as the potential for life; environmental conditions that may have once supported microbial life. A day on Mars, known as a sol, is approximately 24 hours, 39 minutes, and 35.244 seconds long, roughly 40 minutes longer than an Earth Day.

 doi:10.20944/preprints202506.2121.v1

Table 1. Comparison of Earth and Mars Environmental and Physical Conditions [99–101].

Parameters		Earth	Mars
Gravitational acceleration [m/s²]		9.81 (avg.), 9.78(equator)	3.72 (equator)
Diurnal cycle [Earth days]		1	1.02
Rotation period [hours]		23.9345	24.6229
Surface temperature range [°C]		-89– 58	-153– 20
Magnetic vector field (A/m)		24 – 56	0
Atmospheric pressure [bar]		1	6×10^{-3}
Atmospheric composition	O_2	20.9 %	0.16 %
	CO_2	0.03 %	95 %
	CO		0.06
	N_2	78.1 %	2.6 %
	Ar	-	1.9 %
Daily surface radiation [mSv/day]		2 – 3	200

Mars has an axial tilt of 25.2°, which is very similar to Earth's tilt of 23.5°. This means that Mars experiences seasons caused by the same basic principle: as the planet orbits the Sun, different parts of the planet are tilted toward or away from the Sun, leading to seasonal changes in the amount of sunlight a region receives [2]. Seasonal variation on Mars occurs similarly to Earth, with summer and winter in each hemisphere and spring and fall in between. However, because Mars' orbit is more elliptical (elongated), the intensity of the seasons can vary (Figure 2). A Martian year spans approximately 668.6 sols, which is equivalent to about 687 Earth days. Martian months are defined as spanning 30 degrees in solar longitude. Generally, Martian seasons last about twice as long as those on Earth. Due to Mars' orbital eccentricity (elliptical orbit), the lengths of its seasons vary. Southern hemisphere seasons are opposite to those in the northern hemisphere and have slightly different lengths (Table 2). Spring in the northern hemisphere (autumn in the southern) is the longest season at 194 sols. Autumn in the northern hemisphere (spring in the southern) is the shortest at 142 days. Northern winter/southern summer is 154 sols, and northern summer/southern winter is 178 sols. Due to Mars' eccentric orbit and axial tilt, the southern hemisphere experiences colder and longer fall and winter seasons (when farther from the Sun), and hotter and shorter spring and summer seasons (when closer to the Sun), compared to the northern hemisphere.

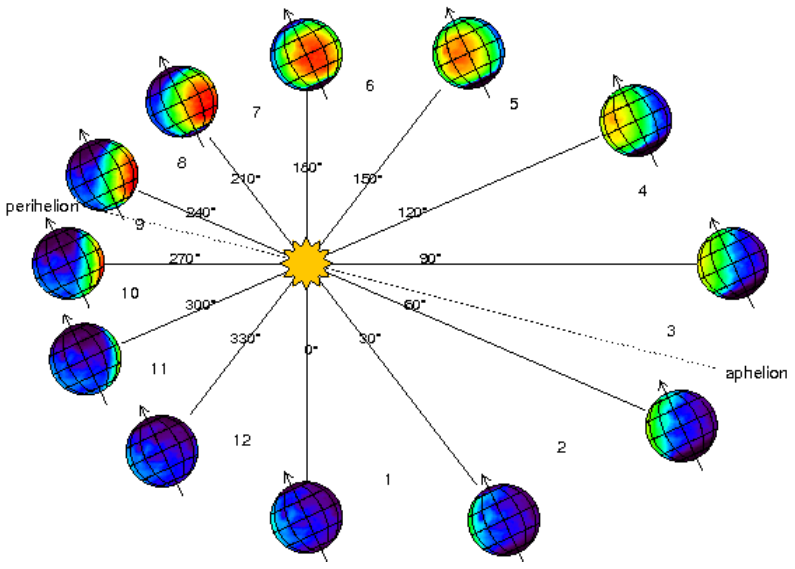

 doi:10.20944/preprints202506.2121.v1

Figure 2. Mars' orbital eccentricity, retrieved with permission from [102].

Table 2. Martian Solar Longitude (Ls) and Seasons, , retrieved with permission from [102].

Month number	Ls range (degrees)	Sol range	duration (in sols)	Specificities
1	0–30	0.0–61.2	61.2	Northern Hemisphere Spring Equinox at Ls=0
2	30–60	61.2–126.6	65.4	
3	60–90	126.6–193.3	66.7	Aphelion (largest Sun-Mars distance) at Ls=71
4	90–120	193.3–257.8	64.5	Northern Hemisphere Summer Solstice at Ls=90
5	120–150	257.8–317.5	59.7	
6	150–180	317.5–371.9	54.4	
7	180–210	371.9–421.6	49.7	Northern Hemisphere Autumn Equinox at Ls=180 Dust Storm Season begins
8	210–240	421.6–468.5	46.9	Dust Storm Season
9	240–270	468.5–514.6	46.1	Perihelion (smallest sun-Mars distance) at Ls=251 Dust Storm Season
10	270–300	514.6–562.0	47.4	Northern hemisphere Winter Solstice at Ls=270 Dust Storm Season
11	300–330	562.0–612.9	50.9	Dust Storm Season
12	330–360	612.9–668.6	55.7	Dust Storm Season ends

Mars differs from Earth in several ways, including a thin atmosphere with predominantly CO_2 and low pressure, freezing temperatures (average -63°C), and a lack of a magnetic field, which leads to severe radiation exposure. These differences between Mars and Earth pose unique challenges for construction materials, needing them to survive severe temperatures, atmospheric conditions, radiation, and dust storms. This section investigates both environmental variables and available resources to identify the elements influencing biocementation on Mars.

3.1. Martian Regolith Chemical Composition and Simulants

3.1.1. Martian Surface Minerology

The layer of loose rock and sediments covering bedrock on planetary surfaces, such the Moon and Mars, is known as planetary regolith. Planetary regolith can be utilised for ISRU or space resource utilisation since it is made up of geologic components like as minerals, amorphous glasses, and native elements. On Earth, regolith forms primarily through the weathering of rocks due to physical, chemical, and biological processes. Physical weathering, such as freeze-thaw cycles, abrasion, and temperature fluctuations, breaks down solid rock into smaller particles. Chemical weathering, driven by water, oxygen, and acids, alters the mineral composition of rocks, leading to soil formation. Biological weathering, caused by plant roots, microorganisms, and burrowing animals, further contributes to the breakdown of rocks and organic material accumulation.

 doi:10.20944/preprints202506.2121.v1

On the Moon and Mars, regolith formation is dominated by different processes due to the lack of liquid water and biological activity. On the Moon, regolith results from billions of years of meteoroid impacts, which pulverize the surface rock into fine dust and fragmented material. This constant bombardment, combined with the harsh vacuum and extreme temperature variations, has created a thick layer of loose, powdery material. On Mars, regolith is shaped by a combination of impact cratering, volcanic activity, wind erosion, and chemical alterations caused by limited atmospheric interactions [103]. Unlike the Moon, Mars has a thin atmosphere, which allows for wind-driven erosion and dust storms that contribute to the redistribution and weathering of surface materials.

Unlike lunar regolith, for which physical samples have been returned to Earth through NASA's Apollo missions, no actual Martian regolith samples are currently available. However, data collected by robotic landers and rovers from multiple Mars missions (Figure 1) have yielded detailed information on the chemical and mineralogical composition of the Martian surface. These findings, derived from in-situ analyses and remote sensing, are synthesized and summarized in Table 3. It is important to note that the values reported here represent equivalent oxide compositions, which reflect the bulk elemental makeup rather than specific mineralogical phases. These oxides are used for standardized geochemical reporting purposes and do not imply that the corresponding free oxide minerals occur in that form on Mars. As expected, there is variability in the chemical composition data obtained from Martian crust, soil, and dust, as well as across different rover missions. These differences arise from spatial heterogeneity on the Martian surface and variations in analytical instrumentation and sampling locations. Nonetheless, the datasets reveal several consistent and distinguishing geochemical characteristics that are highly relevant to the present investigation.

Despite variations in elemental abundances, a comparison between Martian surface geochemistry and the chemical composition of traditional Portland cement indicates that, in theory, all essential precursor compounds required for the formation of cementitious materials are present on Mars. In conventional Portland cement, the primary components including calcium oxide (CaO), silicon dioxide (SiO_2), aluminum oxide (Al_2O_3), and iron oxide (Fe_2O_3) are combined at high temperatures to form key clinker phases, notably tricalcium silicate (C_3S), which is chiefly responsible for the material's binding and strength development properties.

Data from studies of Mars' crust, soil, and dust consistently indicate that SiO_2 (silicon dioxide), also known as silica, is the most abundant compound. This compound plays a crucial role in the formation of cement-like materials, making it an essential component for potential construction on the Martian surface. In the context of biocementation, silica can play a role in the formation of biofilms that help bind particles together. While MICP relies on microbial activity to precipitate calcium carbonate ($CaCO_3$), silica can enhance the strength of the bio-cement by contributing to the mineral matrix.

Calcium oxide (CaO), commonly known as lime, constitutes the highest percentage of Portland cement, ranging from 60 to 67%. As shown in Table 3, however, the chemical composition of Martian regolith contains only a small amount of CaO, varying between 6.1% and 6.92%. Furthermore, CaO is not directly available in large quantities as a pure compound on Mars; instead, it is found as part of various minerals within the Martian regolith. In the context of biocementation on Mars, CaO could potentially be used to provide Ca^{2+} ions, which are essential for the precipitation of $CaCO_3$. However, given its limited availability in Martian regolith and the additional processing steps required to extract Ca^{2+} ions, it may be more practical to rely on Earth-based calcium sources for biocementation processes.

Aluminium oxide (Al_2O_3) plays a secondary yet important role in Portland cement, primarily by accelerating the setting time through its involvement in the formation of calcium aluminate phases. However, this also renders the material more prone to early-stage hydration reactions and associated heat release. In the context of biocementation, Al_2O_3 may influence microbial activity by enhancing biofilm formation or promoting the adhesion of MICP to substrate particles. These interactions could contribute to improved compressive strength and durability of the resulting biocement, suggesting

 doi:10.20944/preprints202506.2121.v1

that Al_2O_3-bearing phases may be beneficial in tailoring cementitious materials for extraterrestrial construction applications, such as on Mars.

Iron(III) oxide (Fe_2O_3) is abundant in Martian regolith and contributes to the planet's characteristic red color. While Fe_2O_3 does not directly participate in the MICP process, certain microorganisms can utilize iron as part of their metabolic pathways, inducing the precipitation of minerals such as magnetite (Fe_3O_4) or siderite ($FeCO_3$) [104,105]. These minerals could further enhance the cementation process. Additionally, due to its resistance to weathering, Fe_2O_3 could improve the long-term durability of biocemented structures on Mars. Given the harsh Martian environment, including factors like radiation and extreme temperature fluctuations, the incorporation of Fe_2O_3 may enhance the biocement's resistance to environmental degradation, thereby increasing its potential for long-term use in construction.

Table 3. Comparison of average chemical compositions of the Martian regolith to cement.

Element/ Compound	Crust [103]	Soil [106]	Dust [106]	Viking 1 [107]	Spirit [108]	Opportunity [109]	Portland Cement ASTM C150 [110]
Weight %							
SiO_2	49.3	46.65 ± 1.2	44.84 ± 0.52	44	45.8 ± 0.44	42.05 ± 4.25	17 – 25
TiO_2	0.98	0.95 ± 0.18	0.95 ± 0.08	0.62	0.81 ± 0.08	1 ± 0.3	–
Al_2O_3	10.5	10.07 ± 0.71	9.32 ± 0.18	7.3	10 ± 0.22	8.3 ± 1.1	≤ 6
Cr_2O_3	0.26	0.39 ± 0.08	0.32 ± 0.04	–	0.35 ± 0.07	–	–
Fe_2O_3	–	4.28 ± 0.74	7.28 ± 0.70	–	–	–	≤ 6
FeO	18.2	12.97 ± 1	10.42 ± 0.11	17.5	15.8 ± 0.36	26.2 ± 0.36	–
MnO	0.36	0.36 ± 0.02	0.33 ± 0.02	-	0.31 ± 0.02	0.31 ± 7.2	–
MgO	9.06	8.12 ± 0.45	7.89 ± 0.32	6	9.3 ± 0.24	6.9 ± 0.5	≤ 6
CaO	6.92	6.70 ± 0.28	6.34 ± 0.20	5.7	6.1 ± 0.27	6.34 ± 1.19	60 – 67
Na_2O	2.97	2.63 ± 0.37	2.56 ± 0.33	–	3.3 ± 0.31	1.6 ± 0.2	–
K_2O	0.45	0.45 ± 0.07	0.48 ± 0.07	< 0.5	0.41 ± 0.03	0.43 ± 0.06	–
P_2O_5	0.90	0.83 ± 0.23	0.92 ± 0.09	–	0.84 ± 0.07	–	–
SO_3	–	4.94 ± 0.74	7.42 ± 0.13	6.7	5.82 ± 0.86	5.91 ± 1.39	< 3
Cl	–	0.59 ± 0.08	0.83 ± 0.05	0.8	0.53 ± 0.13	0.4 ± 0.07	–
Fe^{3+} / Fe_T	–	0.23 ± 0.03	0.39 ± 0.03	–	–	–	–
ppm or µg/g							
Br	–	44 ± 27	28 ± 22	–	40 ± 30	–	–
Ni	337	471 ± 159	552 ± 85	–	450 ± 120	–	–
Zn	320	221 ± 71	404 ± 32	–	300 ± 80	–	–

3.1.2. Martian Regolith Simulants

Simulants' Chemical Composition

As previously mentioned, the NASA/ESA Mars Sample Return (MSR) mission, currently under development, aims to retrieve the first rock and soil samples from Mars, with a projected return in the 2030s. In the absence of actual Martian material, scientists have developed Martian regolith simulants, terrestrial materials engineered to approximate the physical, chemical, and mineralogical

 doi:10.20944/preprints202506.2121.v1

properties of Martian soil. These simulants, including the Mars Mojave Simulant (MMS) [111], the Johnson Space Center Mars-1 Simulant (JSC Mars-1), and the Mars Global Simulant (MGS series) [112] developed by Exolith Lab, are widely used in laboratory studies to investigate planetary construction methods, soil mechanics, plant cultivation, and biocementation. By employing these analogue materials, researchers can evaluate the performance and feasibility of technologies under Mars-like conditions, reducing risk prior to deployment on the Martian surface.

Table 4 presents the chemical composition of various commercially available Martian regolith simulants, along with the corresponding compositional ranges of key oxides as determined from in-situ data collected by Martian rovers and landers, as summarized in Table 3. Since these simulants are intended to replicate the surface regolith (comprising soil and dust), the comparative data in Table 3 exclude contributions from deeper crustal materials. Simulants produced by Exolith Lab are primarily modelled after the Rocknest regolith at Gale Crater, with further compositional adjustments to simulate specific Martian geological environments [112]. For example, MGS-1 (Mars Global Simulant-1) represents a global average composition of Martian regolith. MGS-1C (Clay-Rich Noachian) is enriched in phyllosilicates to reflect early Noachian-era terrains, while MGS-1S (Sulphate-Rich Hydrothermal) incorporates elevated sulphate content to mimic sulphate-bearing hydrothermal deposits. JEZ-1 is formulated to approximate the mineralogical composition of Jezero Crater, including secondary alteration minerals identified by Mars missions.

As expected, SiO_2 (silicon dioxide) is the predominant component in all Martian regolith simulants, with concentrations ranging from 32.6% to 49.4%. However, this range partially exceeds the reported compositional data for Martian surface materials, which lie between 42.05% and 46.65%. Among the simulants, only MMS-2 falls within the typical TiO_2 concentration range, measuring 0.83%. The simulants produced by Exolith Lab generally have lower TiO_2 content, whereas MMS-1 and JSC Mars-1 exceed the typical Martian values, with JSC Mars-1 containing nearly four times the average TiO_2 concentration.

Regarding Al_2O_3, all NASA-produced simulants exceed the expected range, while Exolith simulants remain closer to Martian averages. Cr_2O_3 is detected only in MMS-1 and MMS-2, albeit at levels significantly below the expected Martian concentration. Iron is represented alternately as Fe_2O_3 and FeO across simulants, with Fe_2O_3 consistently exceeding expected Martian values in simulants where it is present. All simulants contain MnO; however, most have concentrations significantly below the expected Martian range, except for JSC Mars-1, which aligns more closely with anticipated levels. The expected MgO content in Martian regolith ranges from 6 to 9.3%, but certain simulants, particularly JEZ-1, display concentrations that considerably exceed this range.

Calcium oxide (CaO) is arguably one of the most critical components in the context of biocementation. On Mars, the CaO content in regolith is typically reported to range between 5.7% and 6.7% by weight. However, most Martian regolith simulants, except for JEZ-1 and JSC Mars-1, contain significantly higher CaO concentrations. For instance, MGS-1S contains approximately 21.39% CaO, which may lead to an overestimation of $CaCO_3$ yield and the apparent efficiency of biocementation processes when using this simulant. This disparity could result in misleading conclusions if the results are directly extrapolated to in-situ Martian conditions. In contrast, the concentrations of sodium oxide (Na_2O) and potassium oxide (K_2O) in several simulants exhibit moderate agreement with Martian regolith data, although some simulants, such as MMS-1 and MMS-2, show slightly elevated Na_2O levels. Notably, MMS-2 closely approximates the sulfur trioxide (SO_3) content reported for Martian regolith, enhancing its potential as a geochemically relevant analog in sulfate-sensitive applications.

 doi:10.20944/preprints202506.2121.v1

Table 4. Comparison of the Martian regolith simulants chemical composition [111–114].

Element/ Compound	Range From Table 3[*] wt %	Exolith				NASA		
		MGS-1 wt %	MGS-1C wt%	MGS-1S wt%	JEZ-1 wt%	MMS-1 wt%	MMS-2 wt%	JSC Mars-1 wt%
SiO_2	42.05–46.65	43.9	43.83	32.6	36.4	49.4	43.8	43.48
TiO_2	0.62–1	0.46	0.39	0.36	0.4	1.09	0.83	3.62
Al_2O_3	7.3–10.07	12.84	10.42	9.59	8	17.10	13.07	22.09
Cr_2O_3	0.32–0.39	-	-	-	-	0.05	0.04	0.03
Fe_2O_3	4.28–7.28	-	7.34	7.79	-	10.87	18.37	16.08
FeO	10.42–26.2	10.60	-	-	11.9	-	-	-
MnO	0.31–0.36	0.11	0.09	0.09	0.1	0.17	0.13	0.26
MgO	6–9.3	14.81	13.47	11.51	25.6	6.08	6.66	4.22
CaO	5.7–6.7	7.91	9.13	21.39	4.6	10.45	7.98	6.05
Na_2O	1.6–3.3	1.49	1.48	1.08	0.9	3.28	2.51	2.34
K_2O	0.41–0.48	0.29	1.44	0.32	0.3	0.48	0.37	0.7
P_2O_5	0.83–0.92	0.17	0.13	0.125	0.1	0.17	0.13	0.78
SO_3	4.94–7.42	-	-	-	-	0.1	6.11	0.31
LOI	-	4.9	10.38	10.76	10	-	-	0
Total	-	97.48	98.11	95.61	98.4	99.24	100	100

[*] calculated from Table 3, excluding data from the Martian crust.

For a more thorough understanding, Figure 3 illustrates the chemical compositions of the selected Martian regolith simulants relative to the average elemental abundances derived from in situ data collected by various Mars landers and rovers. Notably, none of the simulants fully replicate the complex geochemical profile of Martian soil, particularly with respect to sulphates and soluble salts.

A comparison between simulants developed by NASA and those produced by Exolith Lab reveals key compositional differences. For example, Exolith simulants incorporate varying proportions of ferrous oxide (FeO) and ferric oxide (Fe_2O_3), whereas NASA-designed simulants predominantly contain Fe_2O_3 as the principal iron-bearing phase. Additionally, Exolith simulants exhibit elevated magnesium oxide (MgO) content compared to both average Martian regolith and NASA simulants. Conversely, NASA simulants tend to contain significantly more aluminum oxide (Al_2O_3) than both Exolith products and Martian soil averages.

In the context of biocementation, the suitability of a given simulant is highly dependent on the specific microbial pathway being investigated. For instance, biocementation via ureolysis is particularly sensitive to calcium availability. In this regard, the use of Exolith's MGS-1S simulant, which contains approximately four times the CaO content of average Martian regolith, may lead to a substantial overestimation of calcium carbonate precipitation and overall cementation efficiency. Therefore, critical evaluation of simulant composition is essential to avoid over- or underestimation of process viability under actual Martian conditions.

 doi:10.20944/preprints202506.2121.v1

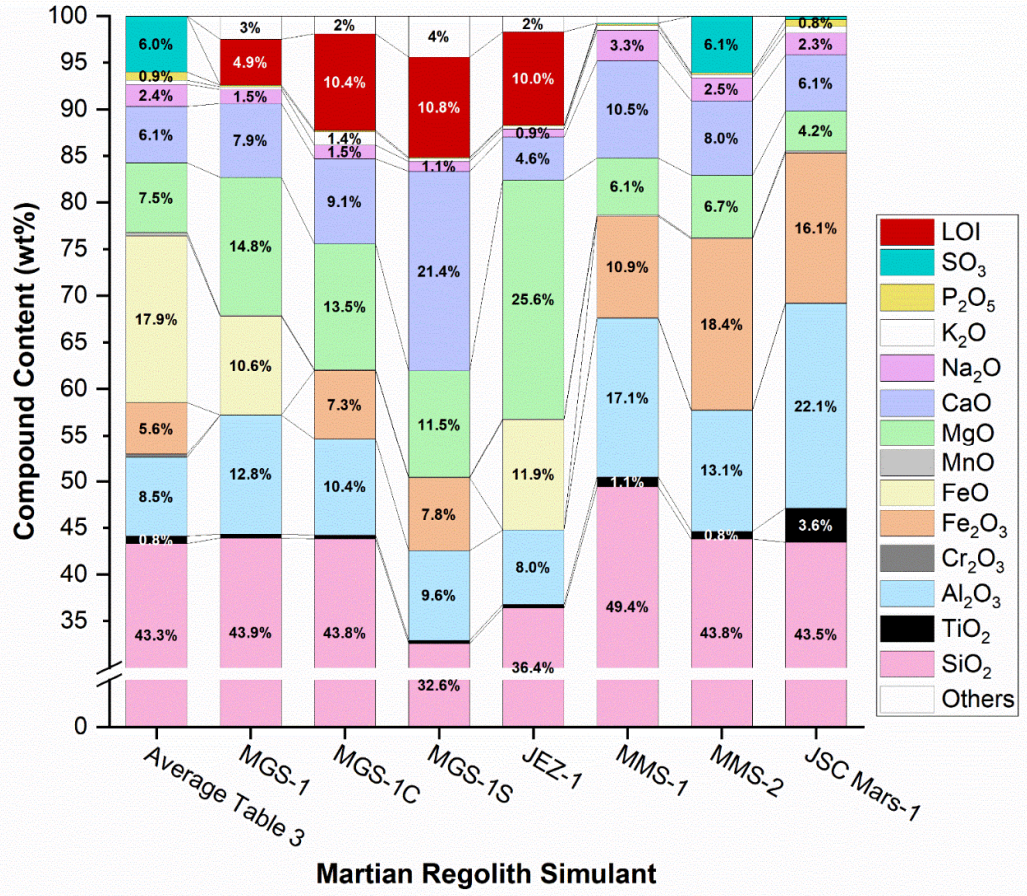

Figure 3. Chemical composition of Martian regolith simulants versus average values collected by landers and rovers.

Particle Size Distribution

Another crucial parameter that influences the properties of concrete, affecting workability, strength, durability, and overall performance, is particle size distribution. In conventional Portland cement, achieving a proper distribution of fine and coarse grains is essential. Fine particles enhance cohesion and reduce segregation, while coarse particles decrease water demand, improving mix stability. Fine particles provide more surface area for bonding, leading to higher strength if properly hydrated, and ensure dense packing, which enhances compressive strength. Coarse particles act as load-bearing components, contributing to compressive strength; however, excessively large aggregates may create voids, reducing overall strength. A well-graded particle distribution, combining both fine and coarse particles, reduces porosity by filling voids, enhancing durability, and improving resistance to freeze-thaw cycles by minimizing water absorption. In contrast, a poorly graded mix, whether excessively fine or coarse, can increase permeability, making the concrete more susceptible to chemical attack and weathering.

In the context of biocementation, the distance between particles acts as nucleation sites for the precipitation of $CaCO_3$ by the bio-cementing agent, making particle size and distribution critical to the effectiveness of biocementation. In mixtures with predominantly fine grains, if the particles are too small, the bio-cementing agent fills the narrow spaces between them, becoming trapped and unable to migrate to new nucleation sites. Conversely, in mixtures with predominantly coarse grains, the larger particle spacing allows microorganisms to move freely through the pores [72]. However, this can lead to excessive voids if microorganisms migrate to new nucleation sites before the pores are properly filled.

 doi:10.20944/preprints202506.2121.v1

Observations from the *Viking*, *Pathfinder*, and *Mars Exploration Rover (MER)* missions indicate that the majority of Martian regolith consists of fine particles smaller than 50 μm [111]. High-resolution imagery from the Viking landers revealed that the dominant aeolian "drift material" typically ranges in particle size from approximately 0.1 to 10 μm, whereas coarser, "blocky material" may reach grain sizes up to 1.5 mm. In addition, all lander missions observed widespread suspended dust in the Martian atmosphere. Atmospheric measurements suggest that airborne dust particles generally fall within the 1–2 μm size range [111].

Figure 4 illustrates the particle size distribution of commercially available Martian regolith simulants. The size distribution of the NASA-designed simulants was quantitatively determined using the "Standard Test Method for Particle-Size Analysis" (ASTM D-422). For particles larger than 75 μm, the size distribution was determined by sieving, while for smaller particles, it was measured using a sedimentation process [111]. The Exolith-designed simulants were analyzed using a CILAS 1190 volumetric particle size analyser in liquid dispersion mode [112]. Table 5 summarizes the percentile values of D10, D50, and D90, calculated from Figure 4, for different Martian regolith simulants.

Bearing in mind that the majority of particles on Mars' surface are smaller than 50 μm, it can be observed that JSC Mars-1 appears to be less similar to Martian regolith, as it contains significantly larger particles, with less than 6% of the particles having dimensions below 50 μm. MMS-1 and MMS-2, on the other hand, have more than 85% and 60%, respectively, of their particles with dimensions below 50 μm. The Exolith-designed Martian simulants exhibit a well-distributed particle size range. MGS-1, MGS-1S, and JEZ-1 contain 50.43%, 42.12%, and 52.19% of particles below 50 μm, respectively. MGS-1C, on the other hand, contains more than 70.62% of particles below 50 μm. Comparing the percentile values of these simulants (Table 5), it can be concluded that, in the context of biocementation, regardless of the specific pathway, MMS-1 may be a better choice from a particle size perspective, as 96.5% of its particles are below 75 μm.

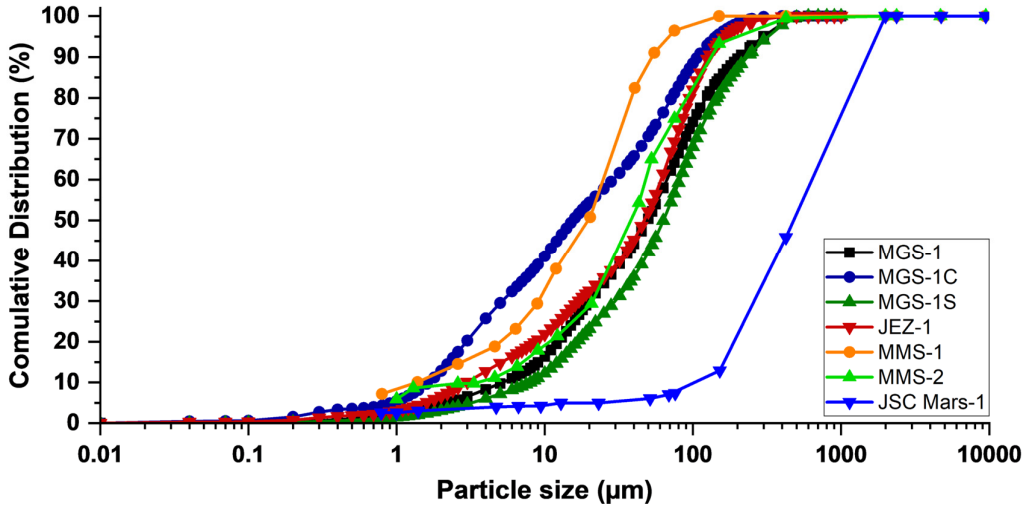

Figure 4. Particle size distribution of different Martian regolith simulants.

Table 5. Percentile values of different Martian regolith simulants.

Quantity	Exolith				NASA		
	MGS-1	MGS-1C	MGS-1S	JEZ-1	MMS-1	MMS-2	JSC Mars-1
D10	5.19	1.64	7.99	2.97	1.45	3.73	111.82
D50	49.3	15.50	63.13	46.92	19.74	39.33	544.42
D90	205.48	107.48	233.17	127.27	53.09	136.63	1703.80

 doi:10.20944/preprints202506.2121.v1

3.2. Water Availability

Water is essential for sustaining human life on Mars and plays a vital role in construction. In particular, biocementation occurs in a water-based solution, and the microorganisms responsible for this process also require water to thrive. Although the Red Planet appears dry, extensive geological evidence suggests that Mars once had a significantly wetter climate, with ancient river valleys, lake beds, and deltas indicating the presence of long-standing bodies of liquid water [115]. The current inventory of water on or near the Martian surface is likely a mere fraction of that on Earth, both in absolute quantities and concentration [103]. Water on Mars exists primarily as ice, with very small amounts as vapour in the atmosphere (~0.03%) and the possibility of liquid water under specific conditions.

Mars has extensive ice caps at both poles, primarily composed of water ice and a seasonal layer of dry ice (CO_2). The volume of polar deposits is approximately 4–5 × 10^6 km^3; nevertheless, the ratio of dust to water remains poorly defined [103]. F.E.G. Butcher [116] provided a comprehensive overview of mid-latitude ice deposits on Mars, highlighting their distribution and potential for in situ resource utilization. Butcher [116] highlighted that Mars' mid-latitudes contain various forms of water ice, including shallow pore ice from atmospheric vapor diffusion, excess ice lenses, thick buried ice layers, and debris-covered glaciers. These deposits collectively hold ice volumes equivalent to a global water layer several meters thick. Most subsurface ice lies within a few hundred meters of the surface. While shallow pore ice forms through vapor diffusion, thick excess ice deposits, reaching hundreds of meters in depth, likely originated from atmospheric snowfall during periods of high obliquity (up to ~35°), later buried by dust and debris. Deeper ice, potentially reaching kilometers in depth, may exist due to groundwater freezing, but current detection methods are limited in identifying such deposits [116].

Data from the Mars Advanced Radar for Subsurface and Ionospheric Sounding (MARSIS) instrument, (Figure 5) , reveal stratified subsurface structures within the Medusae Fossae Formation (MFF) [117]. These internal layers are Estimates suggest that ice-rich material is buried beneath 300–600 m of dry overburden in the MFF, with a total volume equivalent to a global water layer of approximately 1.5 to 2.7 m. This accounts for roughly 30–50% of the total water volume estimated in the North Polar Cap. As previously mentioned, all this water exists in the solid phase, rendering it unsuitable for direct use in biocementation processes, which require liquid water. Although MARSIS has provided evidence of liquid water on Mars, most notably beneath approximately 1.5 kilometres of ice at the base of the South Polar Layered Deposits [118], its inaccessibility presents a major logistical barrier. The technical challenges associated with melting and extracting subsurface ice, as well as the broader considerations for ISRU, fall outside the scope of this study.

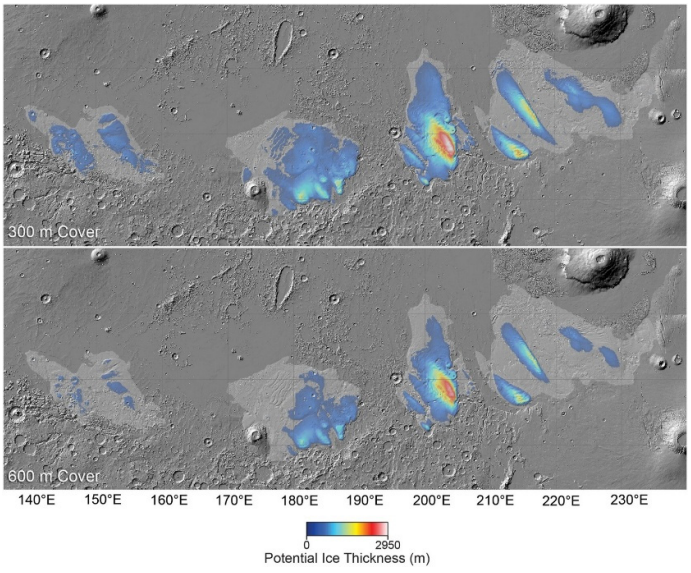

 doi:10.20944/preprints202506.2121.v1

Figure 5. Map of suspected ice at Mars's equator, Mars Express study of the Medusae Fossae Formation (MFF). Retrieved with permission from [117].

3.3. Martian Atmosphere

Mars' weak gravitational field and lack of a protective magnetic field allow the solar wind to strip away atmospheric particles, contributing to the planet's thin atmosphere over time. Mars' thin atmosphere, composed predominantly of carbon dioxide and with a surface pressure about 0.6% of Earth's (Table 1), differs significantly from Earth's atmosphere. In this context, two primary strategies can be considered. The first involves prioritising the selection of anaerobic or facultative anaerobic microbial strains capable of inducing carbonate precipitation under the near-anoxic conditions characteristic of the Martian atmosphere. The second strategy entails engineering localised oxic microenvironments to sustain the metabolic activity of more oxygen-dependent species. This could be achieved through in situ oxygen generation by photosynthetic microorganisms (e.g., cyanobacteria) or by deploying controlled oxygen release systems.

The tenuous atmosphere significantly affects Mars's climatic conditions, including dramatic temperature swings, diurnal and seasonal wind variations, dust storms, liquid water stability, and intense solar radiation. The thin atmosphere provides insufficient insulation, leading to rapid and extreme temperature fluctuations, which are approximately three times greater than those on Earth [119–121]. For instance, daytime temperatures near the equator can reach up to 20°C, while nighttime temperatures can drop to around -125°C. As a consequence of the large day-night temperature fluctuations, Mars' atmosphere experiences diurnal wind variation as well as massive dust storms that can engulf the entire planet for weeks. Without a substantial atmosphere and global magnetic field, Mars' surface is exposed to high levels of cosmic radiation and solar energetic particles [2]. This increased radiation poses significant risks to potential biological organisms and challenges for human exploration. On the other hand, low atmospheric pressure prevents liquid water from existing stably on Mars' surface; it would quickly evaporate or freeze. Apart from water instability on Mars, this section discusses the effect of diurnal temperature fluctuations, solar radiation, and atmospheric pressure, which may compromise bacterial enzymatic activity and, consequently, biocementation efficiency.

3.3.1. Gravity

As mentioned in Table 1 , the gravitational acceleration on Mars is approximately 38% that of Earth's. From a materials science perspective, reduced gravity significantly influences not only the formation of materials but also critical physicochemical processes such as multiphase flow, surface wetting, and interfacial tension. These altered dynamics in turn impact fundamental transport phenomena, namely, mass and heat transfer during solidification. Such changes are particularly consequential for microstructure evolution and pore morphology, both of which are key determinants of material performance and mechanical integrity in cementitious and composite systems [3].

In the context of concrete construction, reduced gravity can offer certain structural advantages by lowering the loads exerted on supporting materials during both construction and long-term use. However, it also poses challenges for the homogeneity and mechanical performance of concrete. On Earth, gravity facilitates the settling of denser constituents like cement, sand, and coarse aggregates while assisting in the upward migration of lighter components such as water and entrained air. This gravitational sorting contributes to a uniform mixture and structural stability [122]. In reduced gravity, these natural separation dynamics are significantly altered or suppressed, potentially resulting in a heterogeneous mix with uneven particle distribution. Such non-uniformity can impair interparticle bonding and increase porosity, ultimately reducing the mechanical strength and durability of the resulting concrete if not properly addressed.

Additionally, water may behave differently, potentially affecting the pore distribution and the way the hydration process unfolds. Water tends to form floating globules rather than evenly

 doi:10.20944/preprints202506.2121.v1

dispersing, leading to higher porosity due to increased voids and microcracks, which can reduce the overall strength of the material. In a unique attempt by NASA, tricalcium silicate (C_3S) was mixed with an aqueous solution and allowed to hydrate in the microgravity environment aboard the International Space Station (ISS) [123]. This study highlighted that bleeding and sedimentation effects are minimised in microgravity, resulting in a paste with a more uniform distribution of hydrated phases and, consequently, a consistent density and porosity. However, the lack of self-weight consolidation and segregation in microgravity led to a 20% increase in porosity, as confirmed by both image analysis and Mercury Intrusion Porosimetry (MIP). Moreover, the pore diameters in microgravity were found to be an order of magnitude larger than those observed in the ground control samples. Figure 6 portrays a comparison of cement porosity distribution under Earth gravity (1g), Lunar gravity (0.17g), and microgravity (μg) environments conducted by NASA [124]. As it can be observed, space-cured concrete had higher porosity and lower strength than Earth-cured concrete, and the microstructure was more heterogeneous, with irregular distribution of hydration products.

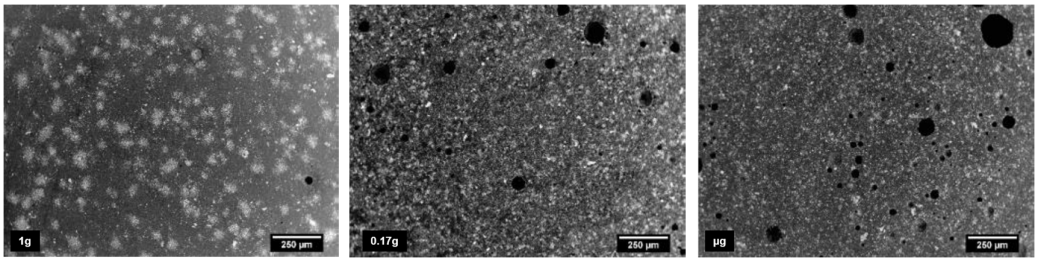

Figure 6. Microscopic image of cement porosity distribution under different gravitation acceleration, retrieved with permission from [124].

In the context of biocementation, reduced gravity introduces additional complexities beyond those encountered with conventional cementitious materials. Microbial behaviour itself may be altered under low-gravity conditions [5]. For instance, microorganisms may experience difficulty adhering to surfaces or spreading uniformly, which can impair biofilm development and reduce the overall efficiency of the biocementation process. Furthermore, the diffusion dynamics of critical gases such as CO_2 and ammonia as well as nutrient transport can deviate significantly from Earth-based conditions. Reduced buoyancy in low gravity may hinder the transport of these gases, which are essential for microbial metabolism and for inducing carbonate precipitation in ureolytic and denitrifying pathways. Additionally, the altered fluid dynamics in reduced gravity affect the distribution and settling behaviour of both microbial suspensions and particulates, potentially leading to heterogeneous carbonate deposition. While some studies, such as Yan et al. [125], reported no significant differences in the extent or characteristics of crude enzyme-induced calcium phosphate precipitation (EICPP) between Earth and microgravity conditions, gravity remains an important factor influencing particle settling and stratification. Settling contributes to spatially uniform nucleation and crystal growth, which are critical for consistent biocementation performance [122]. If not properly controlled, reduced gravity may result in irregular mineral distribution, variable porosity, and diminished mechanical strength in bio-cemented materials. However, it is important to note that, in this context, biocementation may offer distinct advantages over conventional concrete. Microorganisms involved in MICP can continue to precipitate $CaCO_3$ as long as an adequate nutrient supply is maintained. Consequently, if bacterial adhesion to the substrate is sustained, continued calcium carbonate precipitation may lead to a progressive reduction in pore volume over time. This dynamic self-healing capability could result in a denser, less porous matrix compared to conventional cement, which lacks such biological adaptability.

 doi:10.20944/preprints202506.2121.v1

3.3.2. Extreme Temperature Fluctuations

As previously noted, Mars exhibits both diurnal and seasonal temperature variations, with particularly stark contrasts in the southern hemisphere. Due to Mars' elliptical orbit and axial tilt, the southern hemisphere experiences short, intense summers and long, cold winters. Consequently, this region encompasses both the maximum and minimum annual temperature extremes. Figure 7 presents the diurnal temperature profiles at the surface and within the atmosphere of Gale Crater (Latitude = −5.37°, Longitude = 137.81°), located near the Martian equator in the southern hemisphere, during the spring and autumn equinoxes, as well as the summer and winter solstices. Over the annual cycle, temperatures at this site range from approximately −90 °C during the winter solstice to 26.6 °C during the summer solstice. As expected, spring and autumn exhibit intermediate temperature regimes. Prominent diurnal fluctuations are observed across all seasons, with surface temperatures peaking around 1 PM local solar time and dropping sharply during the night. Atmospheric temperatures lag behind, reaching their daily maximum near 5 PM. The disparity between surface and atmospheric temperatures is more evident in warmer seasons, underscoring significant surface heating and the influence of a tenuous or low-density atmosphere. Summer exhibits the most significant temperature difference between day and night, driven by increased solar radiation during the day and reduced cooling at night due to Mars' position near perihelion.

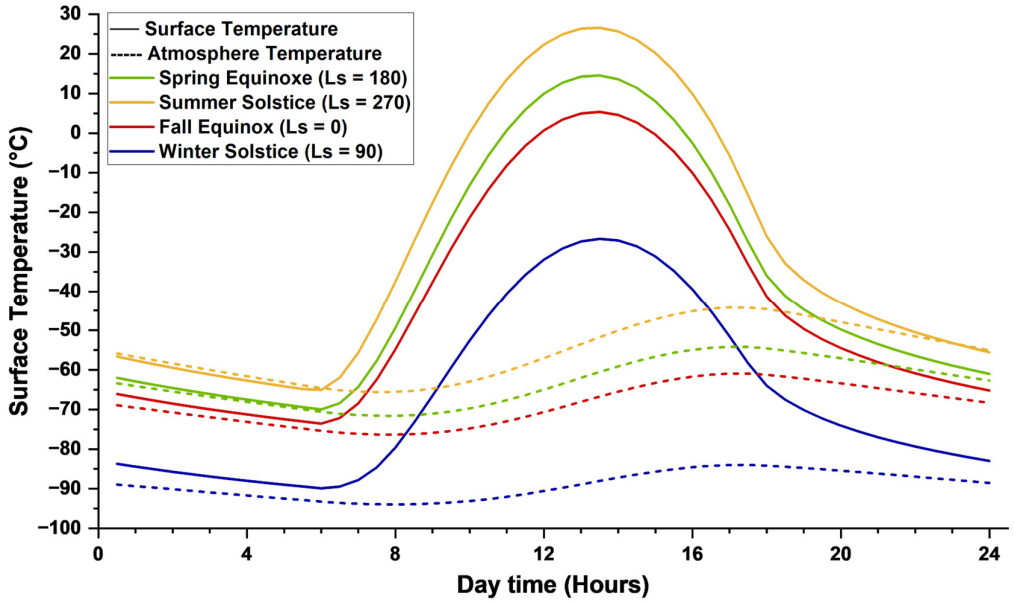

Figure 7. Diurnal surface and atmospheric temperature fluctuations of Gale Crater (southern hemisphere) at the spring and fall equinoxes, as well as the summer and winter solstices, calculated by KRC program.

Temperature plays a critical role in regulating the kinetics of bacterial enzymatic activity during biocementation, much like in other biochemical and chemical processes [72]. Enzyme-mediated reactions, such as ureolysis or carbonic anhydrase activity, are highly temperature-sensitive. Even modest temperature changes of 1–2 °C can lead to reaction rate variations of 10–20%, and it is well-documented that enzyme activity may increase by 50–100% for every 10 °C rise in temperature within the organism's viable range [126,127]. In addition to microbial kinetics, temperature also directly influences mineral precipitation and dissolution dynamics. According to Ostwald's step rule and the temperature-dependent solubility of carbonate minerals, elevated temperatures can alter nucleation pathways, favouring metastable phases or accelerating the dissolution–reprecipitation of less stable polymorphs [128]. Thus, both biological activity and abiotic crystal growth or dissolution processes in biocementation systems are highly sensitive to Martian temperature fluctuations.

 doi:10.20944/preprints202506.2121.v1

In mesophilic bacteria, those adapted to moderate temperatures, enzymatic activity typically declines sharply near 5 °C and can cease altogether below this threshold, effectively halting metabolic processes. As a result, the operational window for biocementation on Mars is severely constrained. For instance, based on diurnal temperature profiles, the temperature remains within the viable range for mesophilic bacterial activity only for short intervals: approximately 1–2 PM in fall, 11:30 AM to 3:30 PM in spring, and 10 AM to 4:30 PM in summer. Psychrophilic bacteria, which are adapted to cold environments, retain enzymatic function at lower temperatures and can continue metabolic activity near 0 °C or slightly below [129,130]. However, due to the extreme diurnal temperature fluctuations on Mars, rising or falling by 15–18°C per hour, even psychrophilic strains would only marginally extend the operational time window for biocementation, likely by no more than one additional hour per sol. Therefore, temperature is a critical parameter for both microbial strain selection and the scheduling of biocementation processes. Achieving effective and sustained carbonate precipitation requires aligning microbial physiology with the narrow thermal windows imposed by Martian diurnal cycles.

3.3.3. High Radiation

Earth's atmosphere, particularly the ozone layer, effectively absorbs and scatters harmful UV radiation, especially UV-B (280–315 nm) and UV-C (<280 nm), shielding the surface from ionising radiation by absorbing a significant portion of it, while the planet's magnetic field deflects charged cosmic rays. In contrast, the surface of Mars, lacking both a substantial atmosphere and a global magnetic field, is exposed to significantly higher levels of radiation compared to Earth. Mars' high radiation levels, encompassing both ultraviolet (UV) and ionising radiation, pose significant challenges to the survival of bacteria intended for biocementation applications. The Radiation Assessment Detector (RAD) aboard the Curiosity Rover provides data on the radiation environment at the Martian surface and serves as an anchor point for modelling subsurface radiation levels. Based on RAD data, D. M. Hassler et al. [99] developed a model demonstrating a significant decrease in radiation dose rate with depth beneath the Martian surface. For instance, at a depth of 1 meter, the estimated Galactic Cosmic Ray (GCR) dose rate is 36.4 mGy/year, which decreases to 1.8 mGy/year at a depth of 3 meters. This suggests that the future of human habitation on Mars may not be on the surface but rather beneath it, where the subsurface provides natural shielding against harmful radiation.

UV radiation is arguably the most extensively studied environmental factor on Mars, primarily from an astrobiology perspective. These investigations have largely focused on microbial survivability under high-radiation conditions. However, such organisms are not necessarily capable of inducing biocementation, as they may lack the metabolic pathways, such as ureolysis or carbonic anhydrase activity. An extensive study examining the survival of spacecraft-associated microorganisms under simulated Martian ultraviolet (UV) radiation, including UVA, UVB, and the full UV spectrum, yielded several critical findings [131,132]. Most notably, *Bacillus pumilus* SAFR-032 was identified as an exceptionally UV-resistant strain, exhibiting up to sixfold greater resistance to simulated Martian UV compared to the laboratory reference strain *Bacillus subtilis* 168. The SAFR-032 strain required approximately an order of magnitude higher UV254 doses for complete inactivation than the thresholds set by standard planetary protection disinfection protocols. Secondly, the study confirmed that the UVC range (200–280 nm) is the primary biocidal component of the Martian UV spectrum. In contrast, UVA and combined UVA+UVB exposures were significantly less effective, necessitating prolonged irradiation to achieve similar reductions in spore viability. Finally, a novel and unexpected protective interaction was observed: co-exposure of *B. subtilis* 168 with viable *B. pumilus* SAFR-032 spores under full-spectrum simulated Martian UV resulted in enhanced survival of the more UV-sensitive strain. This effect was not replicated when SAFR-032 spores were heat-killed prior to co-exposure, suggesting a biologically mediated protective mechanism that warrants further investigation. However, the presence of Martian regolith significantly impacts bacterial survival under ionising radiation. Research involving *Bacillus subtilis* spores revealed that when

 doi:10.20944/preprints202506.2121.v1

covered with Martian regolith, spores were more susceptible to X-ray irradiation, primarily due to interactions between the radiation and the regolith, leading to the formation of secondary electrons and reactive oxygen species[133].

In this context, *Chroococcidiopsis* spp. has shown a remarkable resistance to Martian ultraviolet (UV) radiation primarily attributed to a combination of physiological, genetic, and structural adaptations that enable survival under extreme conditions. Notably, dried biofilms of desert-derived strains have demonstrated the ability to withstand Mars-like UV fluxes and prolonged desiccation, partly due to the constitutive overexpression of UV-damage DNA repair genes and the persistence of ribonucleic acids post-exposure, suggesting a robust molecular response to genotoxic stress [134]. Experimental exposures conducted during the BOSS and BIOMEX missions aboard the EXPOSE-R2 facility in low Earth orbit confirmed that these biofilms can endure simulated Martian atmosphere, vacuum, and intense UVC radiation, particularly when desiccated prior to exposure[135]. The survival of *Chroococcidiopsis* after months of exposure to space and Mars-like conditions, including unfiltered solar UV and freeze–thaw cycling, further underscores the role of desiccation-induced cellular stabilisation mechanisms and protective extracellular matrices in shielding against UV-induced damage[136]. These findings build upon earlier observations that *Chroococcidiopsis* also exhibits high resistance to ionising radiation in the desiccated state, likely due to a shared protective strategy involving macromolecular stabilisation and efficient DNA repair, which together contribute to its candidacy as a model organism for studying microbial persistence on Mars [137].

3.3.4. Low Pressure

Mars' atmospheric pressure, averaging around 6 to 7 millibars (mbar), adds another significant challenge to bacterial survival and activity. To the best of the author's knowledge, there is no existing literature investigating biocementation under low-pressure conditions simulating Mars. However, some studies in the field of astrobiology have explored the survival of bacteria under Martian conditions. T. L. Foster et al. [138] investigated the survival of bacteria in soil samples from Cape Canaveral under simulated Martian conditions, including a pressure of 7 millibars, an atmosphere composed of 99.9% CO_2 and 0.1% O_2, and a freeze-thaw cycle ranging from -65°C to 24°C. The study found that reduced pressure significantly impacted bacterial growth. However, psychrotrophic organisms exhibited an increase of approximately 3 logs within 7 to 14 days when moisture and nutrients were present.

B.J. Berry et al. [139] investigated the growth and survival of two bacterial spacecraft contaminants, *Escherichia coli* and *Serratia liquefaciens*, under simulated Martian conditions. The study exposed the cells to environmental stresses such as high salinity with three salts ($MgCl_2$, $MgSO_4$, NaCl) reported to be present on the surface of Mars, low temperature, and low pressure, and tested them in Mars analogue soils. The results revealed moderate to high growth rates for both *E. coli* and *S. liquefaciens* at low temperatures and in solutions with varying salt concentrations. However, cell densities did not exceed the initial inoculum levels under high salt concentrations and elevated temperatures. While *E. coli* cells were maintained in a Mars analogue soil for 7 days, cell densities failed to increase, and survival was hindered by desiccation, UV irradiation, high salinity, and low pressure.

Additionally, T. Zaccaria et al. [140] examined the survival of *Psychrobacter cryohalolentis* K5, a psychrotolerant bacterium from Siberian permafrost, under simulated Martian surface conditions. Exposed to -12.5°C, 7.1 millibar pressure, and a Mars-like atmospheric composition, the bacterium's survival decreased significantly after 8 hours, particularly due to high UV irradiation. However, when shielded from UV radiation, the bacterium's survivability increased, suggesting that subsurface or shielded environments on Mars might be more conducive to microbial survival.

 doi:10.20944/preprints202506.2121.v1

4. Biocementation on Mars

4.1. Recent Advances in MICP for Construction on Mars

As previously mentioned, very few studies in the literature have investigated the application of biocementation for space construction. Table 6 summarises the only four published articles that employed lunar or Martian regolith simulants as the substrate. It is evident that only one bacterium, *Sporosarcina pasteurii* [60,61], and one microalga, *Thraustochytrium striatum* [62,63], have been studied in this context. Furthermore, the envisioned production methodologies in these studies primarily focus on utilising biocementation for the fabrication of space bricks and the grouting of regolith.

In a study by Dikshit et al. [60], four distinct bacterial growth media were formulated using distilled water and containing peptone, NaCl, mono-potassium phosphate, and urea, with variations introduced through the addition of glucose, guar gum (a plant-derived polysaccharide), and nickel chloride. Guar gum acted as an organic polymer to improve structural integrity, while nickel chloride served as a bio-catalyst to enhance microbial urease activity, thereby facilitating Microbially Induced Calcium Carbonate Precipitation (MICP). Thermogravimetric analysis (TGA) of biocemented specimens incorporating Martian regolith simulant (MGS-1; see Table 4) revealed total calcium carbonate contents of approximately 2.9%, 5.3%, and 7.3% for specimens treated with guar gum, nickel chloride, and their combination, respectively. The carbonate phases formed included the common polymorphs calcite, aragonite, and vaterite. These increases in calcium carbonate content directly correlated with enhancements in compressive strength, yielding values of approximately 1.2 MPa (guar gum only), 2.75 MPa (nickel chloride only), and 3.25 MPa (combined admixture). These results suggest that synergistic use of both the organic polymer and enzymatic cofactor substantially improves the mechanical performance of MICP-treated Martian regolith simulants.

To simulate structural defects, the same research group fabricated geometrically modified bricks using lunar regolith simulants [61]. These bricks incorporated intentional damage features, including a central cylindrical cavity, as well as semi-circular and triangular side notches, produced via a sintering process. The compressive strength of these modified bricks showed a significant reduction with respect to the control specimen (without defect) due to stress concentrations around the artificial cavities. However, after injecting the damaged specimens with a soil slurry incorporating Microbially Induced Calcium Carbonate Precipitation (MICP), a significant recovery in compressive strength was observed, ranging from approximately 28% to 54%. Despite this improvement, the recovered strength did not reach the level of the original, undamaged material [61].

J. Gleaton et al. [62,63] investigated the potential of *Thraustochytrium striatum* as a biocementing agent for the grouting of Mojave Mars Simulant (MMS; see Table 4). The study evaluated several grouting strategies, including simultaneous feeding, sequential feeding, and batch feeding, by varying the recirculation schemes of cell biomass, calcium chloride ($CaCl_2$), and urea through MMS-packed columns. Additional parameters, such as the number of grout recirculation cycles and the post-grouting soaking duration in $CaCl_2$/urea solution, were optimized to enhance biocementation efficiency. X-ray diffraction (XRD) analysis of the treated columns confirmed the formation of calcium carbonate in both calcite and aragonite polymorphic forms. Unconfined compressive strength (UCS) tests revealed a negative correlation between UCS and both extended cell circulation and prolonged post-soaking times. Specifically, UCS values prior to any post-soaking phase were measured at approximately 522 kPa, 472 kPa, 386 kPa, and 409 kPa for cell circulation durations of 3, 6, 9, and 12 hours, respectively. These results identified 3 hours as the optimal duration for cell circulation during the grouting phase [62]. Subsequently, the effect of post-grouting soaking in $CaCl_2$/urea solution was investigated. The highest UCS value—732.40 ± 117.84 kPa—was obtained using a protocol consisting of 3 hours of cell circulation followed by 21 hours of $CaCl_2$/urea circulation, without additional static post-soaking [63]. This protocol was identified as the most effective strategy among those tested.

 doi:10.20944/preprints202506.2121.v1

Table 6. Research progress in exploiting biocementation for space construction.

Ref.	Microorganism	Method	Soil	Environmental Conditions	Medium	Observed Results
[60]	*Sporosarcina pasteurii*	brick	LRS MRS [*]	• 5 days at 32°C • dried in oven at 50°C 24 hours	• KH_2PO_4 • $NiCl_2$ • Calcium lactate • Guar Gum	• Both TGA and mechanical characterization showed a medium with mixture of calcium lactate (50mM), guar gum (1% w/w), $NiCl_2$ (10 mM) results in highest material properties. • TGA showed this medium resulted the highest had $CaCO_3$ precipitation of 7.3% in MRS and 7.1% in LRS. • The compressive strength of MRS and LRS specimens with this medium was evaluate around 3.25 MPa and 5.75 MPa, respectively.
[61]	*Sporosarcina pasteurii*	brick	LRS	• 5 days at 32°C • dried in oven at 60°C	• (NH4)2SO4 • yeast extract • tris buffer	• Compressive strength increase of 28%, 14%, and 55% in bricks with holes, semicircular notches, and V-shaped notches, respectively.
[62]	*Thraustochytrium striatum*	grouting	MRS	• Room temperature • 2 days soaked in medium • 4 days adding medium	• $CaCl_2$ • urea	• The XRD analysis confirmed that the microorganism can precipitate calcite in Martian regolith, • Sequentially and batch grouting of cell biomass and the medium achieved better mechanical properties.
[63]	*Thraustochytrium striatum*	grouting	MRS	• Room temperature • 3-12 hours cell circulation • 0-4 days post grout soaking	• $CaCl_2$ • Calcium acetate • urea	• The XRD analysis confirmed that the microorganism can precipitate $CaCO_3$ (calcite and aragonite) in Martian regolith, • Specimens without post-grout soaking highest mechanical property with an average UCS of 732.40 kPa, • Replacement of $CaCl_2$ with AD VFAs-derived calcium acetate decreased the hydraulic conductivity by 95% compared to the untreated MRS.

[*] LRS: Lunar Regolith Simulant, MRS: Martian Regolith Simulants.

 doi:10.20944/preprints202506.2121.v1

What is particularly notable in these studies is that, although they represent important preliminary steps toward the application of biocementation for Martian construction, they primarily evaluate the suitability of specific microorganisms for the consolidation of Martian regolith simulants under Earth-like environmental conditions. While J. Gleaton et al. [62,63] do mention environmental parameters that may influence microbial viability, the literature reports no experimental data on the performance of biocementation under Mars-analogue environmental conditions, such as low atmospheric pressure, elevated UV radiation, anoxic environments, or pronounced diurnal temperature variations. Consequently, rather than focusing solely on Earth-based biocementation approaches that substitute traditional cementitious substrates with Martian or lunar regolith, the subsequent discussion explores the suitability of different biocementation pathways for Martian applications and addresses strategies to mitigate the challenges posed by the Martian surface environment.

4.2. Promising Biocementation Pathway and Approach

Each biocementation pathway exhibits unique advantages and limitations, rendering it more suitable for specific engineering and environmental applications. Table 7 summarizes the relative reaction rates, required resources, byproducts, environmental conditions, and key microorganisms associated with the biocementation pathways discussed previously.

Table 7. Comparison of different biocementation pathways for Martian construction applications.

Pathway	Speed	Resources	Byproducts	Conditions	Terraforming Phase		
					Before	During	After
Ureolysis	Fast	Urea (urine), Ca^{2+} (regolith)	NH_3 (manageable)	Aerobic/ Anaerobic	✓	✓	✓
Ammonification	Slow	Amino Acids, O_2 Ca^{2+} (regolith)	NH_3 (manageable)	Aerobic/ Anaerobic			✓
Photosynthesis	Slow	CO_2 (atmosphere), light, water	O_2	Anaerobic		✓	✓
Denitrification	Slow	Nitrates (regolith), organic carbon	N_2	Anaerobic		✓	✓
Sulphate Reduction	Slow	Sulphates (regolith), organic carbon	H_2S (toxic)	Anaerobic		✓	✓
Methanogenesis	Slow	CO_2, organic carbon	CH4 (usable)	Anaerobic		✓	✓

Ureolysis enables rapid and efficient calcium carbonate precipitation and is notable for its ability to function across a broad temperature range (~5–50 °C). The use of freeze-dried, urease-positive bacteria further enhances its potential utility, particularly for space missions where long-term microbial storage is necessary. These features provide significant advantages for extraterrestrial construction. However, ureolysis requires a continuous supply of urea, a compound not naturally abundant on Mars. This limitation could be addressed through ISRU, as urea can be extracted from astronaut urine, creating a closed-loop system that repurposes metabolic waste for construction [5]. Another drawback is the generation of ammonia as a byproduct, which may pose toxicity concerns in closed environments. Nevertheless, due to Mars' thin atmosphere and low surface pressure, ammonia is expected to volatilize rapidly after construction is completed. As long as microbial activity ceases when essential resources are depleted, residual ammonia should not pose a long-term risk. Although Martian regolith contains calcium in the form of calcium oxide (CaO), its availability

 doi:10.20944/preprints202506.2121.v1

and extractability remain uncertain, particularly during the early stages of human settlement. Consequently, for the initial implementation of ureolysis-based biocementation, it may be more practical to rely on Earth-supplied calcium sources. This approach ensures a consistent and controlled input of calcium ions necessary for efficient precipitation until reliable in-situ extraction methods are developed. After constructing the first settlement using a terrestrial calcium source as a control, the second settlement can be produced using an ISRU-derived calcium source to enable a direct comparison of performance and feasibility.

Ammonification is, in principle, similar to ureolysis in that both processes generate ammonium ions; however, ammonification occurs at a significantly slower rate. In the context of biocementation, ammonification requires a continuous supply of amino acids (as nitrogen sources), calcium ions, and molecular oxygen. The dependence on these additional elements, combined with the inherently slower rate of ammonium generation and carbonate precipitation, renders ammonification less suitable for early-stage construction in extraterrestrial settlements, where resource efficiency and rapid material formation are critical.

Photosynthesis

Photosynthesis-based biocementation presents a promising approach for surface construction on Mars due to its alignment with the planet's environmental conditions. Leveraging CO_2 from Mars' atmosphere, the process is inherently sustainable when paired with access to sunlight and water. A key advantage of this pathway is the oxygen byproduct, which could supplement life support systems, contributing to a closed-loop habitat design. However, its practical application faces several significant challenges under current Martian conditions While sunlight is required for such processes, intense ultraviolet (UV) radiation on Mars threatens the survival of photosynthetic organisms. UV-shielding membranes would be required to protect them, but doing so would also restrict the visible light required for photosynthesis, producing a significant trade-off. Additionally, the reliance on sunlight restricts its use in shaded or underground habitats, and its slower rate compared to ureolysis limits its suitability for rapid construction. Given these constraints, photosynthesis-based biocementation may prove more feasible and efficient in an early terraformation scenario, where environmental conditions, such as attenuated ultraviolet radiation and a more stable atmospheric composition, would be more conducive to microbial viability and light-driven processes. An alternative strategy could involve leveraging photosynthetic microorganisms to produce oxygen in situ, thereby creating a localised oxic environment that supports the metabolic activity of aerobic biocementing bacteria such as *Sporosarcina pasteurii*. In this approach, a microbial consortium could be engineered wherein the photosynthetic partner sustains the oxygen demand of the ureolytic bacteria, enabling more rapid and efficient calcium carbonate precipitation under otherwise low-oxygen Martian conditions.

Denitrification

Denitrification-based biocementation presents several advantages for Martian applications, particularly in pre- or early-terraformation scenarios. Unlike ureolysis, denitrification does not produce toxic byproducts such as ammonia, making it more environmentally compatible for closed-loop systems. Its independence from light allows for deployment in shaded or subterranean environments, including lava tubes or radiation-shielded habitats, where photosynthesis-based methods are not viable. However, the feasibility of this approach is constrained by the limited natural availability of nitrates and organic carbon on Mars, both of which are essential substrates for the process. These components would need to be imported, synthesised in situ, or supported by engineered bioreactors, increasing system complexity. Additionally, the process proceeds more slowly than ureolysis, which may limit its use in rapid construction scenarios. Despite these challenges, denitrification-based biocementation remains a promising option for Martian construction in controlled environments, offering a biologically cleaner alternative suited to early-stage infrastructure development prior to full-scale terraformation.

Sulphate-reduction

 doi:10.20944/preprints202506.2121.v1

One of the key advantages of the sulphate-reduction pathway lies in the widespread availability of sulphates in Martian regolith, particularly in regions identified by orbiters and rovers such as Meridiani Planum (20-40%). Moreover, sulphate-reduction pathways operate under anaerobic conditions, aligning well with the oxygen-poor Martian environment and enabling their application in subsurface or sealed construction systems. Despite these benefits, several challenges limit the feasibility of SRB-based biocementation on Mars. The process produces hydrogen sulphide (H_2S), a toxic and corrosive gas that poses risks to both microbial viability and habitat safety, necessitating robust containment and gas management systems. Additionally, like denitrifying bacteria, SRBs require a consistent supply of organic carbon to sustain their metabolic activity, which is scarce on Mars and would need to be supplemented. While this method is moderately suitable for Martian use due to the natural abundance of sulphates and compatibility with anoxic conditions, its practicality is constrained by toxic byproduct management and nutrient sourcing challenges, particularly in early or pre-terraformed stages.

Methanogenesis

Methanogenesis-based biocementation, like photosynthesis-driven pathways, utilises atmospheric CO_2 but with the added benefit of producing methane, aligning well with ISRU strategies for rocket fuel. In missions where methane production is already integrated into the system architecture for propulsion or energy storage, this biocementation method could serve as a complementary process, simultaneously contributing to structural material formation and fuel generation. Nevertheless, methanogenesis proceeds slowly, making it less suitable for applications requiring rapid construction. Similar to denitrification and sulphate reduction pathways, it also depends on organic carbon or hydrogen as electron donors, resources that are limited on Mars and would require in-situ production or external supply, adding to system complexity. Despite these constraints, methanogenic biocementation remains a potentially synergistic option for early-stage Martian infrastructure, particularly within ISRU-focused missions or pre-terraformed environments where methane production infrastructure is already in place.

Regardless of specific biocementation pathway, the biocementation approach from an application standpoint can be categorised into four main approaches, each with distinct advantages and limitations:

(i) Use of allochthonous (introduced) or autochthonous (native) viable cells: This approach leverages the metabolic activity of living microorganisms, such as *Sporosarcina pasteurii*, to induce calcium carbonate. Autochthonous microbes are typically well-adapted to the local environment, improving survival and sustainability, while allochthonous strains may offer higher metabolic efficiency or controlled behaviour in engineered systems [36,40,41,50,57,141]. In the context of biocementation on Mars, any bacterium employed for this purpose would be classified as *allochthonous*, given the current absence of known indigenous microbial life. Consequently, challenges arise in maintaining cell viability under the planet's extreme environmental conditions as well as in assessing the potential ecological implications of introducing terrestrial microorganisms into an extraterrestrial environment.

(ii) Cell-free approach: This method involves using microbial extracts, such as urease enzymes or metabolic byproducts, without the presence of living cells [94]. It reduces the risk of microbial proliferation and associated biohazards, while allowing for greater control over the precipitation process. Nonetheless, cost, activity duration, and enzyme stability, in particular, under Martian environmental conditions remain significant limitation.

(iii) Enzyme-Induced Calcium Carbonate Precipitation (EICP): EICP employs purified enzymes, most commonly urease derived from plants or microbes, to catalyse biocementation. This approach is advantageous for its rapid reaction kinetics and absence of living cells, which simplifies application in field conditions. However, enzyme extraction and purification can be costly, and enzyme performance may degrade over time or under extreme conditions [36,38,86,87,142–145].

(iv) Use of Genetically Modified Microorganisms (GMMs): GMMs are engineered to enhance traits such as urease activity, environmental tolerance, or mineral selectivity [146,147]. This approach

 doi:10.20944/preprints202506.2121.v1

holds promise for tailoring microbial performance to specific engineering needs, including low-temperature activity or resistance to salinity. However, concerns over environmental biosafety, regulatory barriers, and potential horizontal gene transfer present notable challenges for field deployment.

From a Martian application perspective, Genetically Modified Microorganisms (GMMs) offer the greatest long-term potential due to their customisability for enhancing traits such as radiation tolerance, urease activity, and metabolic efficiency in extreme environments. Engineered extremophiles could be adapted to thrive under Martian conditions, thereby enabling autonomous and efficient biocementation. However, the use of GMMs introduces significant concerns related to containment, biosafety, and planetary protection, particularly in light of COSPAR guidelines [148] and ethical considerations about forward contamination. Moreover, the development, validation, and regulatory approval of GMMs for extraterrestrial applications may entail substantial delays, pushing their practical deployment into the more distant future. As a result, it is imperative to develop interim strategies that enable early-stage biocementation under Martian conditions. These may include utilizing naturally resilient extremophiles that exhibit innate resistance to radiation, desiccation, and temperature extremes; employing encapsulation technologies to protect microbial agents from environmental stressors; and designing protective physical shields or reactors to create locally controlled environments that enhance cell or enzyme viability. These intermediate solutions would allow experimental implementation of biocementation in near-term Mars missions while ongoing research continues to advance the feasibility and acceptance of GMM-based approaches.

These considerations demonstrate that, due to its rapid reaction kinetics, compatibility with ISRU, and adaptability to Martian environmental conditions, ureolysis is currently the most promising biocementation pathway for early-stage Martian construction. Alternative biocementation mechanisms may still serve valuable long-term or auxiliary roles, particularly in missions involving gradual ISRU integration or post-terraforming scenarios. While photosynthetic microorganisms may not directly contribute to biocementation, they can play a critical supporting role by stabilising the environmental conditions required for the activity of faster-acting, aerobic biocementing species such as *Sporosarcina pasteurii*. A microbial consortium comprising oxygen-producing photosynthetic organisms could help address Mars' oxygen deficiency, thereby enhancing the viability of ureolytic bacteria. Notably, *Chroococcidiopsis* spp. are promising candidates for such consortia: they not only produce oxygen as a metabolic byproduct but also exhibit exceptional resistance to intense UV radiation, thus offering a degree of biological shielding [134–137,149,150]. In such a system, *Chroococcidiopsis* could create a micro-oxic niche that supports the metabolic activity of *Sporosarcina pasteurii*, thereby enabling sustained and effective calcium carbonate precipitation under otherwise hostile Martian surface conditions. The UV resilience of *Chroococcidiopsis* also indirectly enhances the durability of biocemented materials by ensuring microbial viability during early stages of material curing.

Furthermore, this biocementation strategy aligns well with broader ISRU goals and could provide dual utility: as a construction technique and as a functional subsystem supporting critical operations. For instance, CO_2, abundantly available in the Martian atmosphere, serves as a feedstock for both oxygen production via solid oxide electrolysis [151] and plant cultivation in greenhouse systems [152]. In longer-term scenarios, ammonia, a byproduct of ureolysis, may serve as a nitrogen source not only for biocementation but also for Martian agriculture [152,153], facilitating the integration of biotechnological processes across life support and construction domains.

4.3. Road Map Challenges and Mitigation Strategies

Implementing ureolysis-driven biocementation on Mars involves significant challenges due to the planet's extreme environmental stressors, which affect both robotic and crewed missions. The burden of importing materials from Earth will differ between robotic and crewed missions, with robotic missions likely leading early infrastructure development on Mars. A critical issue during early robotic missions is the absence of human-derived waste, specifically urea, which is a key substrate

 doi:10.20944/preprints202506.2121.v1

for ureolytic microbial activity in biocementation. Without this in-situ urea source, the process would require urea transport from Earth, increasing launch mass, cost, and logistical complexity. Unlike other environmental stressors on Mars, which can be mitigated to varying extents through engineering controls, the disparity in gravitational acceleration is an immutable constraint. Therefore, it becomes critically important to strictly regulate and stabilise all other environmental parameters in operational settings. Figure 8 depicts a schematic representation of the roadmap towards implementation of biocementation for Martian construction.

To mitigate Mars' extreme thermal environment and maximise the effectiveness of biocementation, construction activities should ideally be scheduled during the southern hemisphere's summer, which occurs near perihelion. This period offers the longest duration of elevated daytime temperatures, extending the thermal window necessary to sustain bacterial metabolism and enzymatic activity. While the use of psychrophilic bacteria is conceptually appealing, the limited empirical data on their biocementation performance under Martian-like conditions makes them less viable for early-stage deployment. Currently, mesophilic bacteria, whose enzymatic systems are better understood, remain the more practical choice. Notably, the operational advantage of psychrophiles over mesophiles would likely amount to only 1–2 additional hours of feasible activity per sol, owing to the rapid diurnal temperature swings (see Section 3.3.2). This marginal gain could be offset through engineering solutions such as 3D printing systems with thermal regulation or controlled-environment habitats, both of which are explored in later sections.

Upon arrival on Mars, extreme UV irradiation represents the most immediate environmental hazard to microbial viability in biocementation processes. While scheduling construction activities during Martian nighttime or dust storms or within the volcano or crater might theoretically reduce UV exposure, these periods and locations coincide with drastically lower surface temperatures, conditions that inhibit or halt the enzymatic activity of mesophilic bacteria essential for calcium carbonate precipitation. A more viable approach involves physical or biochemical shielding of microbial agents during the active biocementation phase. One strategy is to embed bacterial cultures within protective matrices, such as hydrogels (e.g., alginate) or silica-based biopolymers, which can be engineered to absorb or scatter harmful UV radiation while maintaining permeability for nutrient diffusion and carbonate efflux. However, such encapsulation systems must be precisely tuned to support metabolic exchange and prevent diffusion-limited clogging, especially if calcium carbonate is expected to precipitate near or within the matrix boundary.

Alternatively, the deployment of physical UV-blocking enclosures over the construction site could provide a more immediate and practical solution for mitigating ultraviolet radiation on Mars. This strategy enables an open-system biocementation environment with fewer constraints on gas exchange and diffusion while allowing flexibility in material selection for shielding. Importantly, a UV-blocking membrane integrated into a pressurised geodesic dome could not only attenuate harmful radiation but also mitigate the effects of Mars' extremely low atmospheric pressure [154]. Low pressure on Mars accelerates sublimation and evaporation processes, which can severely disrupt the hydration levels required for microbial metabolism and enzymatic activity critical to biocementation. The pressurised enclosure would enable partial atmospheric control and support the recycling of sublimated or evaporated water within a semi-closed loop system, thereby conserving a vital and limited resource. Although Martian mid-latitude subsurface ice deposits have been identified, their early use remains limited due to uncertainties in accessibility, purity, and the technological challenges associated with extraction, particularly during robotic precursor missions. During crewed missions, recycled water from astronaut waste and perspiration will be prioritised for life-support systems, rendering its allocation to construction processes highly impractical. As such, initial operations may necessitate reliance on Earth-supplied water to ensure consistent and effective biocementation performance.

In summary, considering the operational constraints on the Martian surface and their potential mitigation strategies, a feasible solution for early-stage construction would involve deploying a pressurised, foldable geodesic dome equipped with a UV-shielding membrane to address multiple

 doi:10.20944/preprints202506.2121.v1

environmental challenges simultaneously. By creating a controlled microenvironment, the dome would reduce or eliminate the need for extensive genetic engineering of microbial strains to withstand Martian surface extremes. This protective environment would enhance the predictability and efficiency of biocementation processes during the early phases of extraterrestrial infrastructure development. Moreover, when one structure is completed, the geodesic dome could be relocated to subsequent construction sites, supporting incremental expansion. Its modular and foldable design would allow for repeated deployment, thereby optimizing launch mass and resource utilization while facilitating scalable construction development with minimal additional infrastructure.

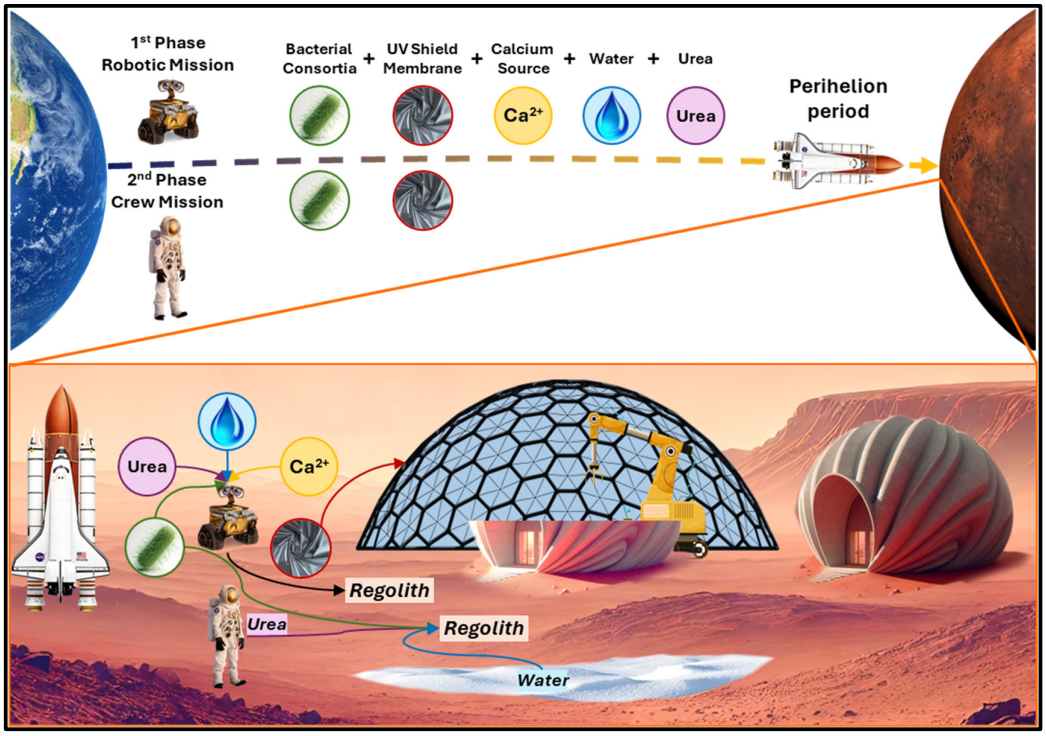

Figure 8. schematic representation of the roadmap for employing biocementation on Mars.

5. Research Gaps and Future Directions

Given the relatively early stage of research into biocementation for Martian construction, conducting a systematic analysis of the research gaps in this domain is essential for building a comprehensive understanding and guiding future investigations. As with other nascent scientific fields, these gaps can be broadly categorised into seven interrelated types [155], which tend to emerge in a semi-systematic and overlapping manner, particularly in complex, interdisciplinary areas such as extraterrestrial biocementation. Identifying and characterising these gaps is a critical step toward developing a strategic research framework capable of accelerating progress toward practical implementation. The seven core gap types, adapted from general models of scientific gap analysis, are outlined below:

1. **Knowledge Gap:** This refers to a fundamental lack of information or comprehensive understanding within the context of biocementation for Martian applications. The primary knowledge gap lies in the absence of an integrated, interdisciplinary overview. Biocementation inherently resides at the intersection of microbiology, materials science, and construction engineering. Even for Earth-based applications, a gap persists in effectively synthesising expertise across these disciplines. The challenge becomes even more complex in the Martian context, where additional considerations in the field of astrobiology, such as microbial survivability in extraterrestrial environments, must be addressed. Researchers with expertise in only one of these domains often find it difficult to fully account for the range of parameters that

 doi:10.20944/preprints202506.2121.v1

influence biocementation on Mars, such as the formulation of appropriate nutrient media for microbial viability, the effects of UV irradiation, extreme thermal fluctuations, or microgravity. This fragmented understanding impedes the design of holistic experimental campaigns that are necessary to systematically address the challenges unique to Martian biocementation.

2. **Theoretical Gap:** The absence of robust underlying theories is primarily rooted in the interdisciplinary complexity of the problem as well as the existing knowledge gap. Biocementation encompasses a wide range of coupled processes, including microbial metabolism, geochemical precipitation, material behaviour, and structural performance, all of which must be reconsidered under the extreme and unprecedented environmental conditions of Mars. Existing theoretical models, which have been developed largely for Earth-based environments, fall short in addressing such extraterrestrial variables. They often neglect critical factors such as the influence of microgravity on microbial growth and biofilm formation, the altered thermodynamics and kinetics of carbonate precipitation at low pressures, and the long-term durability of biocemented structures exposed to Martian radiation and diurnal thermal variations.

In this context, multiphysics finite element modelling (FEM) emerges as a promising tool, coupling biochemical processes with mechanical and thermal simulations that can provide predictive insights into the biocementation under Martian environmental stressors and construction scenarios. Although some existing FEM approaches incorporate bio-coupled, time-dependent behaviours even in terrestrial studies [156,157], such considerations are absent in extraterrestrial modelling efforts. Thus, advancing theoretical models will require both the extension of current computational tools and the generation of foundational experimental data under Mars-analogue conditions.

3. **Empirical Gap:** This engages the absence of observed data or experimental validation, particularly in the context of applying biocementation to extraterrestrial environments. Given the emerging nature of this field, such a gap is expected. However, the empirical gap is further exacerbated by the previously discussed knowledge and theoretical gaps, which hinder the design and implementation of meaningful experiments. The lack of interdisciplinary understanding and robust theoretical models limits the ability to formulate relevant hypotheses and identify critical variables for testing. To bridge this gap, there is a pressing need for a comprehensive experimental framework tailored to Martian conditions (Figure 9). Such a framework should systematically evaluate the performance of biocementation under simulated environmental stressors specific to Mars, including cyclic temperature fluctuations, periodic UV irradiation, reduced gravity, and low atmospheric pressure. Controlled experiments replicating these factors, individually and in combination, are essential to generate empirical data that can validate theoretical models, guide simulation efforts, and inform practical engineering decisions for future Martian construction.

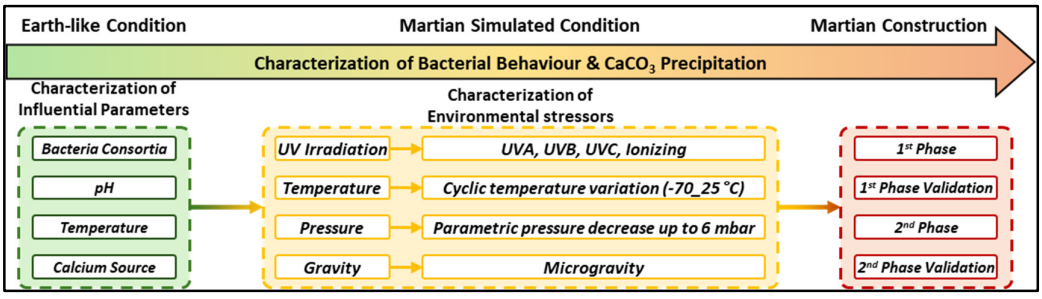

Figure 9. schematic representation of the experimental campaign for characterization of biocementation on Mars.

4. **Evidence Gap:** This type of research gap typically arises after preliminary studies or conceptual proposals have been introduced, yet the resulting data remain inconclusive, inconsistently reproduced, or insufficiently validated through rigorous peer review. In the context of

 doi:10.20944/preprints202506.2121.v1

biocementation for Martian construction, only a limited number of studies [60–63] have reported initial applications of MICP-based approaches using Martian regolith simulants. However, these findings have not been widely replicated, nor have they been tested under mission-relevant environmental constraints. Moreover, critical performance parameters, such as long-term durability under Martian thermal cycling (including freeze–thaw processes), low atmospheric pressure fluctuations, and mechanical stresses arising from structural pressurization or aeolian (wind-driven) forces, remain largely unexplored, even under Earth-based laboratory conditions. Consequently, the current empirical evidence is insufficient to determine whether the issue lies in an unresolved knowledge gap or in a lack of reproducibility.

5. **Population Gap:** In the context of biocementation for Martian applications, this gap refers to the limited diversity of microbial species that have been explored for their suitability in extraterrestrial construction contexts. To date, only two primary organisms *Sporosarcina pasteurii* [60,61] and *Thraustochytrium striatum* [62,63] have been tested for their biocementation potential in Martian regolith simulants. Both species are terrestrial in origin and have not evolved to withstand the harsh environmental stressors found on Mars, such as extreme temperature fluctuations, high UV radiation, low atmospheric pressure, and desiccation.
6. **Methodological Gap:** This type of gap emerges when appropriate, standardized, or sufficiently advanced research methodologies are lacking for the investigation or implementation of a given concept. In the case of biocementation for Martian applications, the methodological gap is particularly significant due to the nascent and interdisciplinary nature of the field, where conventional experimental approaches are not readily transferable to the extreme and atypical conditions of the Martian environment. Most MICP studies conducted to date utilize terrestrial laboratory protocols optimized for Earth's gravity, atmospheric pressure, temperature ranges, and gas composition. These methods fall short in several critical aspects when adapted to Mars-oriented research, such as reliance on simplified regolith simulants, testing under Earth-like environmental conditions, short experimental timeframes, and the absence of integrated modeling–experimentation feedback loops.
7. **Practical-Knowledge Gap**: This gap reflects a disconnect between theoretical or laboratory-based knowledge and the practical application of that knowledge in real-world, or mission-relevant, contexts. Due to the relatively nascent state of the field, this gap remains unresolved in the context of biocementation for Martian applications. To date, the practical implementation of biocementation under simulated Martian environmental conditions has not been systematically explored, even within controlled laboratory settings. As a result, no experimental data yet exists to assess the feasibility or performance of MICP-based construction under conditions approximating the Martian surface.

CRediT authorship contribution statement: Shiva Khoshtinat: Conceptualization, Investigation, Formal analysis, Writing - Original Draft, Writing - Review & Editing, Visualization.

Declaration of Competing Interest: The author declares no known competing financial interests or personal relationships that could have appeared to influence the work reported in this paper.

Data Availability: Data will be made available on request.

Acknowledgements: Not applicable.

References

1. Z. Chen, L. Zhang, Y. Tang, B. Chen, Pioneering lunar habitats through comparative analysis of in-situ concrete technologies: A critical review, Constr. Build. Mater. 435 (2024) 136833. https://doi.org/10.1016/j.conbuildmat.2024.136833.
2. F. Neukart, Towards sustainable horizons: A comprehensive blueprint for Mars colonization, Heliyon 10 (2024) e26180. https://doi.org/10.1016/j.heliyon.2024.e26180.

 doi:10.20944/preprints202506.2121.v1

3. M.Z. Naser, Extraterrestrial construction materials, Prog. Mater. Sci. 105 (2019) 100577. https://doi.org/10.1016/j.pmatsci.2019.100577.
4. Y. Wang, L. Hao, Y. Li, Q. Sun, M. Sun, Y. Huang, Z. Li, D. Tang, Y. Wang, L. Xiao, In-situ utilization of regolith resource and future exploration of additive manufacturing for lunar/martian habitats: A review, Appl. Clay Sci. 229 (2022) 106673. https://doi.org/10.1016/j.clay.2022.106673.
5. H. Zuo, S. Ni, M. Xu, An assumption of in situ resource utilization for "bio-bricks" in space exploration, Front. Mater. 10 (2023) 1155643. https://doi.org/10.3389/fmats.2023.1155643.
6. K.W. Farries, P. Visintin, S.T. Smith, P. Van Eyk, Sintered or melted regolith for lunar construction: state-of-the-art review and future research directions, Constr. Build. Mater. 296 (2021) 123627. https://doi.org/10.1016/j.conbuildmat.2021.123627.
7. H.A. Toutanji, S. Evans, R.N. Grugel, Performance of lunar sulfur concrete in lunar environments, Constr. Build. Mater. 29 (2012) 444–448. https://doi.org/10.1016/j.conbuildmat.2011.10.041.
8. L. Cai, L. Ding, H. Luo, X. Yi, Preparation of autoclave concrete from basaltic lunar regolith simulant: Effect of mixture and manufacture process, Constr. Build. Mater. 207 (2019) 373–386. https://doi.org/10.1016/j.conbuildmat.2019.02.146.
9. L. Chen, T. Wang, F. Li, S. Zhou, Preparation of geopolymer for in-situ pavement construction on the moon utilizing minimal additives and human urine in lunar regolith simulant, Front. Mater. 11 (2024) 1413432. https://doi.org/10.3389/fmats.2024.1413432.
10. J.J. Sokołowska, P. Woyciechowski, M. Kalinowski, Rheological Properties of Lunar Mortars, Appl. Sci. 11 (2021) 6961. https://doi.org/10.3390/app11156961.
11. Q. Cui, T. Wang, G. Gu, R. Zhang, T. Zhao, Z. Huang, G. Wang, F. Chen, Ultraviolet and thermal dual-curing assisted extrusion-based additive manufacturing of lunar regolith simulant for in-site construction on the Moon, Constr. Build. Mater. 425 (2024) 136010. https://doi.org/10.1016/j.conbuildmat.2024.136010.
12. MARS GLOBAL SURVEYOR RAW DATA SET - CRUISE V1.0, (2025). https://catalog.data.gov/dataset/mars-global-surveyor-raw-data-set-cruise-v1-0-ad4ef?utm_source=chatgpt.com (accessed May 17, 2025).
13. PDS Geosciences Node Data and Services: 2001 Mars Odyssey, (n.d.). https://pds-geosciences.wustl.edu/missions/odyssey/ (accessed May 17, 2025).
14. PDS Geosciences Node Data and Services: ESA Mars Express Mission, (n.d.). https://pds-geosciences.wustl.edu/missions/mars_express/default.htm (accessed May 17, 2025).
15. EMM Science Data Center, (n.d.). https://sdc.emiratesmarsmission.ae/ (accessed May 13, 2025).
16. PDS Geosciences Node Data and Services: Viking Lander, (n.d.). https://pds-geosciences.wustl.edu/missions/vlander/index.htm (accessed May 17, 2025).
17. PDS Geosciences Node Data and Services: Mars Pathfinder, (n.d.). https://pds-geosciences.wustl.edu/missions/mpf/index.htm (accessed May 17, 2025).
18. PDS Geosciences Node Data and Services: Phoenix Mission, (n.d.). https://pds-geosciences.wustl.edu/missions/phoenix/index.htm (accessed May 17, 2025).
19. PDS Geosciences Node Data and Services: Mars Science Laboratory (MSL) Mission, (n.d.). https://pds-geosciences.wustl.edu/missions/msl/index.htm (accessed May 17, 2025).
20. PDS Geosciences Node Data and Services: InSight Mission, (n.d.). https://pds-geosciences.wustl.edu/missions/insight/index.htm (accessed May 17, 2025).
21. Mars Orbiters and Landers, (n.d.). https://pds-atmospheres.nmsu.edu/data_and_services/atmospheres_data/MARS/mars_lander.html (accessed May 13, 2025).
22. PDS Geosciences Node Data and Services: Mars 2020 Mission, (n.d.). https://pds-geosciences.wustl.edu/missions/mars2020/index.htm (accessed May 17, 2025).
23. Map of NASA's Mars Landing Sites - NASA Science, (2020). https://science.nasa.gov/resource/map-of-nasas-mars-landing-sites/ (accessed March 27, 2025).
24. M.Z. Naser, Q. Chen, Extraterrestrial Construction in Lunar and Martian Environments, in: Earth Space 2021, American Society of Civil Engineers, Virtual Conference, 2021: pp. 1200–1207. https://doi.org/10.1061/9780784483374.111.

 doi:10.20944/preprints202506.2121.v1

25. L. Wan, R. Wendner, G. Cusatis, A novel material for in situ construction on Mars: experiments and numerical simulations, Constr. Build. Mater. 120 (2016) 222–231. https://doi.org/10.1016/j.conbuildmat.2016.05.046.
26. M.H. Shahsavari, M.M. Karbala, S. Iranfar, V. Vandeginste, Martian and lunar sulfur concrete mechanical and chemical properties considering regolith ingredients and sublimation, Constr. Build. Mater. 350 (2022) 128914. https://doi.org/10.1016/j.conbuildmat.2022.128914.
27. H.A. Lowenstam, S. Weiner, H.A. Lowenstam, S. Weiner, On Biomineralization, Oxford University Press, Oxford, New York, 1989.
28. S. Mann, Biomineralization Principles and Concepts in Bioinorganic Materials Chemistry, Oxford University Press, 2001. https://doi.org/10.1093/oso/9780198508823.002.0001.
29. S. Khoshtinat, J. Long-Fox, S.M.J. Hosseini, From Earth to Mars: A Perspective on Exploiting Biomineralization for Martian Construction, (2025). https://doi.org/10.20944/preprints202506.1171.v1.
30. A.I. Omoregie, E.A. Palombo, D.E.L. Ong, P.M. Nissom, A feasible scale-up production of Sporosarcina pasteurii using custom-built stirred tank reactor for in-situ soil biocementation, Biocatal. Agric. Biotechnol. 24 (2020) 101544. https://doi.org/10.1016/j.bcab.2020.101544.
31. K.M.N.S. Wani, B.A. Mir, An Experimental Study on the Bio-cementation and Bio-clogging Effect of Bacteria in Improving Weak Dredged Soils, Geotech. Geol. Eng. 39 (2021) 317–334. https://doi.org/10.1007/s10706-020-01494-0.
32. A.M. Sharaky, N.S. Mohamed, M.E. Elmashad, N.M. Shredah, Application of microbial biocementation to improve the physico-mechanical properties of sandy soil, Constr. Build. Mater. 190 (2018) 861–869. https://doi.org/10.1016/j.conbuildmat.2018.09.159.
33. K. Xu, M. Huang, C. Xu, J. Zhen, G. Jin, H. Gong, Assessment of the bio-cementation effect on shale soil using ultrasound measurement, Soils Found. 63 (2023) 101249. https://doi.org/10.1016/j.sandf.2022.101249.
34. A.A. Dubey, K. Ravi, A. Mukherjee, L. Sahoo, M.A. Abiala, N.K. Dhami, Biocementation mediated by native microbes from Brahmaputra riverbank for mitigation of soil erodibility, Sci. Rep. 11 (2021) 15250. https://doi.org/10.1038/s41598-021-94614-6.
35. L. Cheng, M.A. Shahin, R. Cord-Ruwisch, Bio-cementation of sandy soil using microbially induced carbonate precipitation for marine environments, Géotechnique 64 (2014) 1010–1013. https://doi.org/10.1680/geot.14.T.025.
36. H. Abdel-Aleem, T. Dishisha, A. Saafan, A.A. AbouKhadra, Y. Gaber, Biocementation of soil by calcite/aragonite precipitation using *Pseudomonas azotoformans* and *Citrobacter freundii* derived enzymes, RSC Adv. 9 (2019) 17601–17611. https://doi.org/10.1039/C9RA02247C.
37. J. Yin, J.-X. Wu, K. Zhang, M.A. Shahin, L. Cheng, Comparison between MICP-Based Bio-Cementation Versus Traditional Portland Cementation for Oil-Contaminated Soil Stabilisation, Sustainability 15 (2022) 434. https://doi.org/10.3390/su15010434.
38. P.J. Venda Oliveira, J.P.G. Neves, Effect of Organic Matter Content on Enzymatic Biocementation Process Applied to Coarse-Grained Soils, J. Mater. Civ. Eng. 31 (2019) 04019121. https://doi.org/10.1061/(ASCE)MT.1943-5533.0002774.
39. V.S. Whiffin, L.A. van Paassen, M.P. Harkes, Microbial carbonate precipitation as a soil improvement technique, Geomicrobiol. J. 24 (2007) 417–423. https://doi.org/10.1080/01490450701436505.
40. D. Mujah, M.A. Shahin, L. Cheng, State-of-the-Art Review of Biocementation by Microbially Induced Calcite Precipitation (MICP) for Soil Stabilization, Geomicrobiol. J. 34 (2017) 524–537. https://doi.org/10.1080/01490451.2016.1225866.
41. A.I. Omoregie, E.A. Palombo, P.M. Nissom, Bioprecipitation of calcium carbonate mediated by ureolysis: A review, Environ. Eng. Res. 26 (2021). https://doi.org/10.4491/eer.2020.379.
42. D.M. Iqbal, L.S. Wong, S.Y. Kong, Bio-Cementation in Construction Materials: A Review, Materials 14 (2021) 2175. https://doi.org/10.3390/ma14092175.
43. N.N.T. Huynh, K. Imamoto, C. Kiyohara, A Study on Biomineralization using *Bacillus Subtilis* Natto for Repeatability of Self-Healing Concrete and Strength Improvement, J. Adv. Concr. Technol. 17 (2019) 700–714. https://doi.org/10.3151/jact.17.700.

 doi:10.20944/preprints202506.2121.v1

44. M. Bagga, C. Hamley-Bennett, A. Alex, B.L. Freeman, I. Justo-Reinoso, I.C. Mihai, S. Gebhard, K. Paine, A.D. Jefferson, E. Masoero, I.D. Ofiţeru, Advancements in bacteria based self-healing concrete and the promise of modelling, Constr. Build. Mater. 358 (2022) 129412. https://doi.org/10.1016/j.conbuildmat.2022.129412.
45. N.N.T. Huynh, N.M. Phuong, N.P.A. Toan, N.K. Son, Bacillus Subtilis HU58 Immobilized in Micropores of Diatomite for Using in Self-healing Concrete, Procedia Eng. 171 (2017) 598–605. https://doi.org/10.1016/j.proeng.2017.01.385.
46. N.N.T. Huynh, K. Imamoto, C. Kiyohara, Biomineralization Analysis and Hydration Acceleration Effect in Self-healing Concrete using *Bacillus subtilis natto*, J. Adv. Concr. Technol. 20 (2022) 609–623. https://doi.org/10.3151/jact.20.609.
47. N. Huynh, K. Imamoto, C. Kiyohara, Compressive Strength Improvement and Water Permeability of Self-Healing Concrete Using Bacillus Subtilis Natto, in: XV Int. Conf. Durab. Build. Mater. Compon. EBook Proc., CIMNE, 2020. https://doi.org/10.23967/dbmc.2020.024.
48. S. Joshi, S. Goyal, M.S. Reddy, Corn steep liquor as a nutritional source for biocementation and its impact on concrete structural properties, J. Ind. Microbiol. Biotechnol. 45 (2018) 657–667. https://doi.org/10.1007/s10295-018-2050-4.
49. M. Wu, X. Hu, Q. Zhang, D. Xue, Y. Zhao, Growth environment optimization for inducing bacterial mineralization and its application in concrete healing, Constr. Build. Mater. 209 (2019) 631–643. https://doi.org/10.1016/j.conbuildmat.2019.03.181.
50. S. Krishnapriya, D.L. Venkatesh Babu, P.A. G., Isolation and identification of bacteria to improve the strength of concrete, Microbiol. Res. 174 (2015) 48–55. https://doi.org/10.1016/j.micres.2015.03.009.
51. M.J. Castro-Alonso, L.E. Montañez-Hernandez, M.A. Sanchez-Muñoz, M.R. Macias Franco, R. Narayanasamy, N. Balagurusamy, Microbially Induced Calcium Carbonate Precipitation (MICP) and Its Potential in Bioconcrete: Microbiological and Molecular Concepts, Front. Mater. 6 (2019) 126. https://doi.org/10.3389/fmats.2019.00126.
52. R. Devrani, A.A. Dubey, K. Ravi, L. Sahoo, Applications of bio-cementation and bio-polymerization for aeolian erosion control, J. Arid Environ. 187 (2021) 104433. https://doi.org/10.1016/j.jaridenv.2020.104433.
53. S.M. Fattahi, A. Soroush, N. Huang, Biocementation Control of Sand against Wind Erosion, J. Geotech. Geoenvironmental Eng. 146 (2020) 04020045. https://doi.org/10.1061/(ASCE)GT.1943-5606.0002268.
54. A.A. Dubey, R. Devrani, K. Ravi, N.K. Dhami, A. Mukherjee, L. Sahoo, Experimental investigation to mitigate aeolian erosion via biocementation employed with a novel ureolytic soil isolate, Aeolian Res. 52 (2021) 100727. https://doi.org/10.1016/j.aeolia.2021.100727.
55. S.M.A. Zomorodian, H. Ghaffari, B.C. O'Kelly, Stabilisation of crustal sand layer using biocementation technique for wind erosion control, Aeolian Res. 40 (2019) 34–41. https://doi.org/10.1016/j.aeolia.2019.06.001.
56. X. Xu, H. Guo, M. Li, X. Deng, Bio-cementation improvement via CaCO3 cementation pattern and crystal polymorph: A review, Constr. Build. Mater. 297 (2021) 123478. https://doi.org/10.1016/j.conbuildmat.2021.123478.
57. K.D. Mutitu, M.O. Munyao, M.J. Wachira, R. Mwirichia, K.J. Thiong'o, M.J. Marangu, Effects of biocementation on some properties of cement-based materials incorporating *Bacillus Species* bacteria – a review, J. Sustain. Cem.-Based Mater. 8 (2019) 309–325. https://doi.org/10.1080/21650373.2019.1640141.
58. B. Aytekin, A. Mardani, Ş. Yazıcı, State-of-art review of bacteria-based self-healing concrete: Biomineralization process, crack healing, and mechanical properties, Constr. Build. Mater. 378 (2023) 131198. https://doi.org/10.1016/j.conbuildmat.2023.131198.
59. M. Amran, A.M. Onaizi, R. Fediuk, N.I. Vatin, R.S. Muhammad Rashid, H. Abdelgader, T. Ozbakkaloglu, Self-Healing Concrete as a Prospective Construction Material: A Review, Materials 15 (2022) 3214. https://doi.org/10.3390/ma15093214.
60. R. Dikshit, N. Gupta, A. Dey, K. Viswanathan, A. Kumar, Microbial induced calcite precipitation can consolidate martian and lunar regolith simulants, PLOS ONE 17 (2022) e0266415. https://doi.org/10.1371/journal.pone.0266415.

 doi:10.20944/preprints202506.2121.v1

61. N. Gupta, R. Kulkarni, A.R. Naik, K. Viswanathan, A. Kumar, Bacterial bio-cementation can repair space bricks, Front. Space Technol. 6 (2025) 1550526. https://doi.org/10.3389/frspt.2025.1550526.
62. J. Gleaton, R. Xiao, Z. Lai, N. McDaniel, C.A. Johnstone, B. Burden, Q. Chen, Y. Zheng, Biocementation of Martian Regolith Simulant with In Situ Resources, in: Earth Space 2018, American Society of Civil Engineers, Cleveland, Ohio, 2018: pp. 591–599. https://doi.org/10.1061/9780784481899.056.
63. J. Gleaton, Z. Lai, R. Xiao, Q. Chen, Y. Zheng, Microalga-induced biocementation of martian regolith simulant: Effects of biogrouting methods and calcium sources, Constr. Build. Mater. 229 (2019) 116885. https://doi.org/10.1016/j.conbuildmat.2019.116885.
64. T. Perez-Gonzalez, C. Jimenez-Lopez, A.L. Neal, F. Rull-Perez, A. Rodriguez-Navarro, A. Fernandez-Vivas, E. Iañez-Pareja, Magnetite biomineralization induced by *Shewanella oneidensis*, Geochim. Cosmochim. Acta 74 (2010) 967–979. https://doi.org/10.1016/j.gca.2009.10.035.
65. L. Fu, S.-W. Li, Z.-W. Ding, J. Ding, Y.-Z. Lu, R.J. Zeng, Iron reduction in the DAMO/*Shewanella oneidensis* MR-1 coculture system and the fate of Fe(II), Water Res. 88 (2016) 808–815. https://doi.org/10.1016/j.watres.2015.11.011.
66. L. Kong, S. Sun, B. Liu, S. Zhang, X. Zhang, Y. Liu, H. Yang, Y. Zhao, Microbial treatment of aluminosilicate solid wastes: A green technique for cementitious materials, J. Clean. Prod. 499 (2025) 145216. https://doi.org/10.1016/j.jclepro.2025.145216.
67. C. Zhang, F. Li, Magnesium isotope fractionation during carbonate precipitation associated with bacteria and extracellular polymeric substances, Int. Biodeterior. Biodegrad. 173 (2022) 105441. https://doi.org/10.1016/j.ibiod.2022.105441.
68. H. Porter, A. Mukherjee, R. Tuladhar, N.K. Dhami, Life Cycle Assessment of Biocement: An Emerging Sustainable Solution?, Sustainability 13 (2021) 13878. https://doi.org/10.3390/su132413878.
69. A. Bandyopadhyay, A. Saha, D. Ghosh, B. Dam, A.K. Samanta, S. Dutta, Microbial repairing of concrete & its role in CO2 sequestration: a critical review, Beni-Suef Univ. J. Basic Appl. Sci. 12 (2023) 7. https://doi.org/10.1186/s43088-023-00344-1.
70. C. Wu, J. Chu, S. Wu, Y. Hong, 3D characterization of microbially induced carbonate precipitation in rock fracture and the resulted permeability reduction, Eng. Geol. 249 (2019) 23–30. https://doi.org/10.1016/j.enggeo.2018.12.017.
71. Y. Wang, K. Soga, J.T. Dejong, A.J. Kabla, Microscale Visualization of Microbial-Induced Calcium Carbonate Precipitation Processes, J. Geotech. Geoenvironmental Eng. 145 (2019). https://doi.org/10.1061/(ASCE)GT.1943-5606.0002079.
72. S. Khoshtinat, Advancements in Exploiting Sporosarcina pasteurii as Sustainable Construction Material: A Review, Sustainability 15 (2023) 13869. https://doi.org/10.3390/su151813869.
73. N. Erdmann, D. Strieth, Influencing factors on ureolytic microbiologically induced calcium carbonate precipitation for biocementation, World J. Microbiol. Biotechnol. 39 (2022) 61. https://doi.org/10.1007/s11274-022-03499-8.
74. C. Dupraz, P.T. Visscher, Microbial lithification in marine stromatolites and hypersaline mats, Trends Microbiol. 13 (2005) 429–438. https://doi.org/10.1016/j.tim.2005.07.008.
75. L.A. van Paassen, C.M. Daza, M. Staal, D.Y. Sorokin, W. van der Zon, Mark.C.M. van Loosdrecht, Potential soil reinforcement by biological denitrification, Ecol. Eng. 36 (2010) 168–175. https://doi.org/10.1016/j.ecoleng.2009.03.026.
76. J.T. DeJong, B.M. Mortensen, B.C. Martinez, D.C. Nelson, Bio-mediated soil improvement, Ecol. Eng. 36 (2010) 197–210. https://doi.org/10.1016/j.ecoleng.2008.12.029.
77. T. Zhu, M. Dittrich, Carbonate Precipitation through Microbial Activities in Natural Environment, and Their Potential in Biotechnology: A Review, Front. Bioeng. Biotechnol. 4 (2016). https://doi.org/10.3389/fbioe.2016.00004.
78. V. Achal, A. Mukherjee, D. Kumari, Q. Zhang, Biomineralization for sustainable construction – A review of processes and applications, Earth-Sci. Rev. 148 (2015) 1–17. https://doi.org/10.1016/j.earscirev.2015.05.008.
79. B. Krajewska, Urease-aided calcium carbonate mineralization for engineering applications: A review, J. Adv. Res. 13 (2018) 59–67. https://doi.org/10.1016/j.jare.2017.10.009.

 doi:10.20944/preprints202506.2121.v1

80. H.L. Mobley, R.P. Hausinger, Microbial ureases: significance, regulation, and molecular characterization, Microbiol. Rev. (1989). https://doi.org/10.1128/mr.53.1.85-108.1989.
81. D. Ariyanti, Feasibility of Using Microalgae for Biocement Production through Biocementation, J. Bioprocess. Biotech. 02 (2012). https://doi.org/10.4172/2155-9821.1000111.
82. J. Gleaton, Z. Lai, R. Xiao, Q. Chen, Y. Zheng, Microalga-induced biocementation of martian regolith simulant: Effects of biogrouting methods and calcium sources, Constr. Build. Mater. 229 (2019) 116885. https://doi.org/10.1016/j.conbuildmat.2019.116885.
83. L.J. Mapstone, M.N. Leite, S. Purton, I.A. Crawford, L. Dartnell, Cyanobacteria and microalgae in supporting human habitation on Mars, Biotechnol. Adv. 59 (2022) 107946. https://doi.org/10.1016/j.biotechadv.2022.107946.
84. C. Fang, D. Kumari, X. Zhu, V. Achal, Role of fungal-mediated mineralization in biocementation of sand and its improved compressive strength, Int. Biodeterior. Biodegrad. 133 (2018) 216–220. https://doi.org/10.1016/j.ibiod.2018.07.013.
85. P.G. Oktafiani, H. Putra, Erizal, D.H.Y. Yanto, Application of technical grade reagent in soybean-crude urease calcite precipitation (SCU-CP) method for soil improvement technique, Phys. Chem. Earth Parts ABC 128 (2022) 103292. https://doi.org/10.1016/j.pce.2022.103292.
86. D. Guan, Y. Zhou, M.A. Shahin, H. Khodadadi Tirkolaei, L. Cheng, Assessment of urease enzyme extraction for superior and economic bio-cementation of granular materials using enzyme-induced carbonate precipitation, Acta Geotech. 18 (2023) 2263–2279. https://doi.org/10.1007/s11440-022-01727-x.
87. A. Miftah, H. Khodadadi Tirkolaei, H. Bilsel, Biocementation of Calcareous Beach Sand Using Enzymatic Calcium Carbonate Precipitation, Crystals 10 (2020) 888. https://doi.org/10.3390/cryst10100888.
88. Y.J. Phua, A. Røyne, Bio-cementation through controlled dissolution and recrystallization of calcium carbonate, Constr. Build. Mater. 167 (2018) 657–668. https://doi.org/10.1016/j.conbuildmat.2018.02.059.
89. G.A.M. Metwally, M. Mahdy, A.E.-R.H. Abd El-Raheem, Performance of Bio Concrete by Using Bacillus Pasteurii Bacteria, Civ. Eng. J. 6 (2020) 1443–1456. https://doi.org/10.28991/cej-2020-03091559.
90. Z. Tian, X. Tang, Z. Xiu, Z. Xue, The Spatial Distribution of Microbially Induced Carbonate Precipitation in Sand Column with Different Grouting Strategies, J. Mater. Civ. Eng. 35 (2023) 04022437. https://doi.org/10.1061/(ASCE)MT.1943-5533.0004615.
91. M.V.S. Rao, V.S. Reddy, Ch. Sasikala, Performance of Microbial Concrete Developed Using Bacillus Subtilus JC3, J. Inst. Eng. India Ser. A 98 (2017) 501–510. https://doi.org/10.1007/s40030-017-0227-x.
92. G. Kaur, N.K. Dhami, S. Goyal, A. Mukherjee, M.S. Reddy, Utilization of carbon dioxide as an alternative to urea in biocementation, Constr. Build. Mater. 123 (2016) 527–533. https://doi.org/10.1016/j.conbuildmat.2016.07.036.
93. C. Fang, J. He, V. Achal, G. Plaza, Tofu Wastewater as Efficient Nutritional Source in Biocementation for Improved Mechanical Strength of Cement Mortars, Geomicrobiol. J. 36 (2019) 515–521. https://doi.org/10.1080/01490451.2019.1576804.
94. B. Perito, M. Marvasi, C. Barabesi, G. Mastromei, S. Bracci, M. Vendrell, P. Tiano, A Bacillus subtilis cell fraction (BCF) inducing calcium carbonate precipitation: Biotechnological perspectives for monumental stone reinforcement, J. Cult. Herit. 15 (2014) 345–351. https://doi.org/10.1016/j.culher.2013.10.001.
95. K.A. Joshi, M.B. Kumthekar, V.P. Ghodake, Bacillus Subtilis Bacteria Impregnation in Concrete for Enhancement in Compressive Strength, 03 (n.d.).
96. Z.-F. Xue, W.-C. Cheng, M.M. Rahman, L. Wang, Y.-X. Xie, Immobilization of Pb(II) by *Bacillus megaterium*-based microbial-induced phosphate precipitation (MIPP) considering bacterial phosphorolysis ability and Ca-mediated alleviation of lead toxicity, Environ. Pollut. 355 (2024) 124229. https://doi.org/10.1016/j.envpol.2024.124229.
97. S.M. Andersen, H.S. Mortensen, R. Bossi, C.S. Jacobsen, Isolation and characterisation of Rhodococcus erythropolis TA57 able to degrade the triazine amine product from hydrolysis of sulfonylurea pesticides in soils, Syst. Appl. Microbiol. 24 (2001) 262–266. https://doi.org/10.1078/0723-2020-00036.
98. C. Jansson, T. Northen, Calcifying cyanobacteria—the potential of biomineralization for carbon capture and storage, Curr. Opin. Biotechnol. 21 (2010) 365–371. https://doi.org/10.1016/j.copbio.2010.03.017.

 doi:10.20944/preprints202506.2121.v1

99. D.M. Hassler, C. Zeitlin, R.F. Wimmer-Schweingruber, B. Ehresmann, S. Rafkin, J.L. Eigenbrode, D.E. Brinza, G. Weigle, S. Böttcher, E. Böhm, S. Burmeister, J. Guo, J. Köhler, C. Martin, G. Reitz, F.A. Cucinotta, M.-H. Kim, D. Grinspoon, M.A. Bullock, A. Posner, J. Gómez-Elvira, A. Vasavada, J.P. Grotzinger, M.S. Team, O. Kemppinen, D. Cremers, J.F. Bell, L. Edgar, J. Farmer, A. Godber, M. Wadhwa, D. Wellington, I. McEwan, C. Newman, M. Richardson, A. Charpentier, L. Peret, P. King, J. Blank, M. Schmidt, S. Li, R. Milliken, K. Robertson, V. Sun, M. Baker, C. Edwards, B. Ehlmann, K. Farley, J. Griffes, H. Miller, M. Newcombe, C. Pilorget, M. Rice, K. Siebach, K. Stack, E. Stolper, C. Brunet, V. Hipkin, R. Léveillé, G. Marchand, P.S. Sánchez, L. Favot, G. Cody, A. Steele, L. Flückiger, D. Lees, A. Nefian, M. Martin, M. Gailhanou, F. Westall, G. Israël, C. Agard, J. Baroukh, C. Donny, A. Gaboriaud, P. Guillemot, V. Lafaille, E. Lorigny, A. Paillet, R. Pérez, M. Saccoccio, C. Yana, C. Armiens-Aparicio, J.C. Rodríguez, I.C. Blázquez, F.G. Gómez, S. Hettrich, A.L. Malvitte, M.M. Jiménez, J. Martínez-Frías, J. Martín-Soler, F.J. Martín-Torres, A.M. Jurado, L. Mora-Sotomayor, G.M. Caro, S.N. López, V. Peinado-González, J. Pla-García, J.A.R. Manfredi, J.J. Romeral-Planelló, S.A.S. Fuentes, E.S. Martinez, J.T. Redondo, R. Urqui-O'Callaghan, M.-P.Z. Mier, S. Chipera, J.-L. Lacour, P. Mauchien, J.-B. Sirven, H. Manning, A. Fairén, A. Hayes, J. Joseph, S. Squyres, R. Sullivan, P. Thomas, A. Dupont, A. Lundberg, N. Melikechi, A. Mezzacappa, T. Berger, D. Matthia, B. Prats, E. Atlaskin, M. Genzer, A.-M. Harri, H. Haukka, H. Kahanpää, J. Kauhanen, O. Kemppinen, M. Paton, J. Polkko, W. Schmidt, T. Siili, C. Fabre, J. Wray, M.B. Wilhelm, F. Poitrasson, K. Patel, S. Gorevan, S. Indyk, G. Paulsen, S. Gupta, D. Bish, J. Schieber, B. Gondet, Y. Langevin, C. Geffroy, D. Baratoux, G. Berger, A. Cros, C. d'Uston, O. Forni, O. Gasnault, J. Lasue, Q.-M. Lee, S. Maurice, P.-Y. Meslin, E. Pallier, Y. Parot, P. Pinet, S. Schröder, M. Toplis, É. Lewin, W. Brunner, E. Heydari, C. Achilles, D. Oehler, B. Sutter, M. Cabane, D. Coscia, G. Israël, C. Szopa, G. Dromart, F. Robert, V. Sautter, S. Le Mouélic, N. Mangold, M. Nachon, A. Buch, F. Stalport, P. Coll, P. François, F. Raulin, S. Teinturier, J. Cameron, S. Clegg, A. Cousin, D. DeLapp, R. Dingler, R.S. Jackson, S. Johnstone, N. Lanza, C. Little, T. Nelson, R.C. Wiens, R.B. Williams, A. Jones, L. Kirkland, A. Treiman, B. Baker, B. Cantor, M. Caplinger, S. Davis, B. Duston, K. Edgett, D. Fay, C. Hardgrove, D. Harker, P. Herrera, E. Jensen, M.R. Kennedy, G. Krezoski, D. Krysak, L. Lipkaman, M. Malin, E. McCartney, S. McNair, B. Nixon, L. Posiolova, M. Ravine, A. Salamon, L. Saper, K. Stoiber, K. Supulver, J. Van Beek, T. Van Beek, R. Zimdar, K.L. French, K. Iagnemma, K. Miller, R. Summons, F. Goesmann, W. Goetz, S. Hviid, M. Johnson, M. Lefavor, E. Lyness, E. Breves, M.D. Dyar, C. Fassett, D.F. Blake, T. Bristow, D. DesMarais, L. Edwards, R. Haberle, T. Hoehler, J. Hollingsworth, M. Kahre, L. Keely, C. McKay, M.B. Wilhelm, L. Bleacher, W. Brinckerhoff, D. Choi, P. Conrad, J.P. Dworkin, M. Floyd, C. Freissinet, J. Garvin, D. Glavin, D. Harpold, A. Jones, P. Mahaffy, D.K. Martin, A. McAdam, A. Pavlov, E. Raaen, M.D. Smith, J. Stern, F. Tan, M. Trainer, M. Meyer, M. Voytek, R.C. Anderson, A. Aubrey, L.W. Beegle, A. Behar, D. Blaney, F. Calef, L. Christensen, J.A. Crisp, L. DeFlores, B. Ehlmann, J. Feldman, S. Feldman, G. Flesch, J. Hurowitz, I. Jun, D. Keymeulen, J. Maki, M. Mischna, J.M. Morookian, T. Parker, B. Pavri, M. Schoppers, A. Sengstacken, J.J. Simmonds, N. Spanovich, M.D.L.T. Juarez, C.R. Webster, A. Yen, P.D. Archer, J.H. Jones, D. Ming, R.V. Morris, P. Niles, E. Rampe, T. Nolan, M. Fisk, L. Radziemski, B. Barraclough, S. Bender, D. Berman, E.N. Dobrea, R. Tokar, D. Vaniman, R.M.E. Williams, A. Yingst, K. Lewis, L. Leshin, T. Cleghorn, W. Huntress, G. Manhès, J. Hudgins, T. Olson, N. Stewart, P. Sarrazin, J. Grant, E. Vicenzi, S.A. Wilson, V. Hamilton, J. Peterson, F. Fedosov, D. Golovin, N. Karpushkina, A. Kozyrev, M. Litvak, A. Malakhov, I. Mitrofanov, M. Mokrousov, S. Nikiforov, V. Prokhorov, A. Sanin, V. Tretyakov, A. Varenikov, A. Vostrukhin, R. Kuzmin, B. Clark, M. Wolff, S. McLennan, O. Botta, D. Drake, K. Bean, M. Lemmon, S.P. Schwenzer, R.B. Anderson, K. Herkenhoff, E.M. Lee, R. Sucharski, M.Á.D.P. Hernández, J.J.B. Ávalos, M. Ramos, C. Malespin, I. Plante, J.-P. Muller, R. Navarro-González, R. Ewing, W. Boynton, R. Downs, M. Fitzgibbon, K. Harshman, S. Morrison, W. Dietrich, O. Kortmann, M. Palucis, D.Y. Sumner, A. Williams, G. Lugmair, M.A. Wilson, D. Rubin, B. Jakosky, T. Balic-Zunic, J. Frydenvang, J.K. Jensen, K. Kinch, A. Koefoed, M.B. Madsen, S.L.S. Stipp, N. Boyd, J.L. Campbell, R. Gellert, G. Perrett, I. Pradler, S. VanBommel, S. Jacob, T. Owen, S. Rowland, E. Atlaskin, H. Savijärvi, C.M. García, R. Mueller-Mellin, J.C. Bridges, T. McConnochie, M. Benna, H. Franz, H. Bower, A. Brunner, H. Blau, T. Boucher, M. Carmosino, S. Atreya, H. Elliott, D. Halleaux, N. Rennó, M. Wong, R. Pepin, B. Elliott, J. Spray, L. Thompson, S. Gordon, H. Newsom, A. Ollila, J. Williams, P. Vasconcelos, J. Bentz, K. Nealson, R. Popa, L.C. Kah, J. Moersch, C. Tate, M. Day, G. Kocurek, B. Hallet, R. Sletten, R. Francis, E. McCullough, E. Cloutis,

 doi:10.20944/preprints202506.2121.v1

I.L. Ten Kate, R. Kuzmin, R. Arvidson, A. Fraeman, D. Scholes, S. Slavney, T. Stein, J. Ward, J. Berger, J.E. Moores, Mars' Surface Radiation Environment Measured with the Mars Science Laboratory's Curiosity Rover, Science 343 (2014) 1244797. https://doi.org/10.1126/science.1244797.

100. Temperatures Across Our Solar System - NASA Science, (2023). https://science.nasa.gov/solar-system/temperatures-across-our-solar-system/ (accessed March 15, 2025).
101. With Mars Methane Mystery Unsolved, Curiosity Serves Scientists a New One: Oxygen - NASA, (2019). https://www.nasa.gov/missions/with-mars-methane-mystery-unsolved-curiosity-serves-scientists-a-new-one-oxygen/ (accessed March 15, 2025).
102. Martian Seasons and Solar Longitude Ls, (n.d.). https://www-mars.lmd.jussieu.fr/mars/time/solar_longitude.html (accessed March 27, 2025).
103. S.R. Taylor, S. McLennan, Planetary Crusts: Their Composition, Origin and Evolution, Cambridge University Press, Cambridge, 2008. https://doi.org/10.1017/CBO9780511575358.
104. Y. Roh, C.-L. Zhang, H. Vali, R.J. Lauf, J. Zhou, T.J. Phelps, Biogeochemical and Environmental Factors in Fe Biomineralization: Magnetite and Siderite Formation, Clays Clay Miner. 51 (2003) 83–95. https://doi.org/10.1346/CCMN.2003.510110.
105. X. Han, F. Wang, S. Zheng, H. Qiu, Y. Liu, J. Wang, N. Menguy, E. Leroy, J. Bourgon, A. Kappler, F. Liu, Y. Pan, J. Li, Morphological, Microstructural, and In Situ Chemical Characteristics of Siderite Produced by Iron-Reducing Bacteria, Environ. Sci. Technol. 58 (2024) 11016–11026. https://doi.org/10.1021/acs.est.3c10988.
106. R.V. Morris, G. Klingelhöfer, C. Schröder, D.S. Rodionov, A. Yen, D.W. Ming, P.A. De Souza, T. Wdowiak, I. Fleischer, R. Gellert, B. Bernhardt, U. Bonnes, B.A. Cohen, E.N. Evlanov, J. Foh, P. Gütlich, E. Kankeleit, T. McCoy, D.W. Mittlefehldt, F. Renz, M.E. Schmidt, B. Zubkov, S.W. Squyres, R.E. Arvidson, Mössbauer mineralogy of rock, soil, and dust at Meridiani Planum, Mars: Opportunity's journey across sulfate-rich outcrop, basaltic sand and dust, and hematite lag deposits, J. Geophys. Res. Planets 111 (2006) 2006JE002791. https://doi.org/10.1029/2006JE002791.
107. B.C. Clark, A.K. Baird, R.J. Weldon, D.M. Tsusaki, L. Schnabel, M.P. Candelaria, Chemical composition of Martian fines, J. Geophys. Res. Solid Earth 87 (1982) 10059–10067. https://doi.org/10.1029/JB087iB12p10059.
108. R. Gellert, R. Rieder, R.C. Anderson, J. Brückner, B.C. Clark, G. Dreibus, T. Economou, G. Klingelhöfer, G.W. Lugmair, D.W. Ming, S.W. Squyres, C. d'Uston, H. Wänke, A. Yen, J. Zipfel, Chemistry of Rocks and Soils in Gusev Crater from the Alpha Particle X-ray Spectrometer, Science 305 (2004) 829–832. https://doi.org/10.1126/science.1099913.
109. R. Rieder, R. Gellert, R.C. Anderson, J. Brückner, B.C. Clark, G. Dreibus, T. Economou, G. Klingelhöfer, G.W. Lugmair, D.W. Ming, S.W. Squyres, C. d'Uston, H. Wänke, A. Yen, J. Zipfel, Chemistry of Rocks and Soils at Meridiani Planum from the Alpha Particle X-ray Spectrometer, Science 306 (2004) 1746–1749. https://doi.org/10.1126/science.1104358.
110. ASTM C150, (n.d.). https://compass.astm.org/document/?contentCode=ASTM%7CC0150_C0150M-24%7Cen-US (accessed March 15, 2025).
111. G.H. Peters, W. Abbey, G.H. Bearman, G.S. Mungas, J.A. Smith, R.C. Anderson, S. Douglas, L.W. Beegle, Mojave Mars simulant—Characterization of a new geologic Mars analog, Icarus 197 (2008) 470–479. https://doi.org/10.1016/j.icarus.2008.05.004.
112. J.M. Long-Fox, D.T. Britt, Characterization of planetary regolith simulants for the research and development of space resource technologies, Front. Space Technol. 4 (2023) 1255535. https://doi.org/10.3389/frspt.2023.1255535.
113. K.M. Cannon, D.T. Britt, T.M. Smith, R.F. Fritsche, D. Batcheldor, Mars global simulant MGS-1: A Rocknest-based open standard for basaltic martian regolith simulants, Icarus 317 (2019) 470–478. https://doi.org/10.1016/j.icarus.2018.08.019.
114. Martian Regolith Simulants, Space Resour. Technol. (n.d.). https://spaceresourcetech.com/collections/martian-simulants (accessed March 16, 2025).
115. D.P. Mason, L.A. Scuderi, Interweaving recurring slope lineae on Mars: Do they support a wet hypothesis?, Icarus 419 (2024) 115980. https://doi.org/10.1016/j.icarus.2024.115980.

 doi:10.20944/preprints202506.2121.v1

116. F.E.G. Butcher, Water Ice at Mid-Latitudes on Mars, in: Oxf. Res. Encycl. Planet. Sci., 2022. https://doi.org/10.1093/acrefore/9780190647926.013.239.
117. T.R. Watters, B.A. Campbell, C.J. Leuschen, G.A. Morgan, A. Cicchetti, R. Orosei, J.J. Plaut, Evidence of Ice-Rich Layered Deposits in the Medusae Fossae Formation of Mars, Geophys. Res. Lett. 51 (2024) e2023GL105490. https://doi.org/10.1029/2023GL105490.
118. R. Orosei, S.E. Lauro, E. Pettinelli, A. Cicchetti, M. Coradini, B. Cosciotti, F. Di Paolo, E. Flamini, E. Mattei, M. Pajola, F. Soldovieri, M. Cartacci, F. Cassenti, A. Frigeri, S. Giuppi, R. Martufi, A. Masdea, G. Mitri, C. Nenna, R. Noschese, M. Restano, R. Seu, Radar evidence of subglacial liquid water on Mars, Science 361 (2018) 490–493. https://doi.org/10.1126/science.aar7268.
119. S. Fan, F. Forget, M.D. Smith, S. Guerlet, K.M. Badri, S.A. Atwood, R.M.B. Young, C.S. Edwards, P.R. Christensen, J. Deighan, H.R. Al Matroushi, A. Bierjon, J. Liu, E. Millour, Migrating Thermal Tides in the Martian Atmosphere During Aphelion Season Observed by EMM/EMIRS, Geophys. Res. Lett. 49 (2022) e2022GL099494. https://doi.org/10.1029/2022GL099494.
120. D. Atri, N. Abdelmoneim, D.B. Dhuri, M. Simoni, Diurnal variation of the surface temperature of Mars with the Emirates Mars Mission: a comparison with Curiosity and Perseverance rover measurements, Mon. Not. R. Astron. Soc. Lett. 518 (2023) L1–L6. https://doi.org/10.1093/mnrasl/slac094.
121. Y. Wang, S. Jin, Diurnal temperature cycle models and performances on Martian surface using in-situ and satellite data, Planet. Space Sci. (2025) 106100. https://doi.org/10.1016/j.pss.2025.106100.
122. P.J. Collins, R.J. Thomas, A. Radlińska, Influence of gravity on the micromechanical properties of portland cement and lunar regolith simulant composites, Cem. Concr. Res. 172 (2023) 107232. https://doi.org/10.1016/j.cemconres.2023.107232.
123. J. Moraes Neves, P.J. Collins, R.P. Wilkerson, R.N. Grugel, A. Radlińska, Microgravity Effect on Microstructural Development of Tri-calcium Silicate (C3S) Paste, Front. Mater. 6 (2019). https://doi.org/10.3389/fmats.2019.00083.
124. Microgravity Investigation of Cement Solidification (MICS) - NASA Science, (n.d.). https://science.nasa.gov/image-detail/mics/ (accessed March 22, 2025).
125. Z. Yan, K. Nakashima, C. Takano, S. Kawasaki, Kitchen Waste Bone-Driven Enzyme-Induced Calcium Phosphate Precipitation under Microgravity for Space Biocementation, Biogeotechnics (2024) 100156. https://doi.org/10.1016/j.bgtech.2024.100156.
126. M.E. Peterson, R.M. Daniel, M.J. Danson, R. Eisenthal, The dependence of enzyme activity on temperature: determination and validation of parameters, Biochem. J. 402 (2007) 331–337. https://doi.org/10.1042/BJ20061143.
127. S. Khoshtinat, State-of-the-Art Review of Aliphatic Polyesters and Polyolefins Biodeterioration by Microorganisms: From Mechanism to Characterization, Corros. Mater. Degrad. 4 (2023) 542–572. https://doi.org/10.3390/cmd4040029.
128. Y. Wang, Y. Wang, K. Soga, J.T. DeJong, A.J. Kabla, Microscale investigations of temperature-dependent microbially induced carbonate precipitation (MICP) in the temperature range 4–50 °C, Acta Geotech. 18 (2023) 2239–2261. https://doi.org/10.1007/s11440-022-01664-9.
129. G. Feller, E. Narinx, J.L. Arpigny, Z. Zekhnini, J. Swings, C. Gerday, Temperature dependence of growth, enzyme secretion and activity of psychrophilic Antarctic bacteria, Appl. Microbiol. Biotechnol. 41 (1994) 477–479. https://doi.org/10.1007/BF01982539.
130. C. Gerday, Psychrophily and Catalysis, Biology 2 (2013) 719–741. https://doi.org/10.3390/biology2020719.
131. D.A. Newcombe, A.C. Schuerger, J.N. Benardini, D. Dickinson, R. Tanner, K. Venkateswaran, Survival of spacecraft-associated microorganisms under simulated martian UV irradiation, Appl. Environ. Microbiol. 71 (2005) 8147–8156. https://doi.org/10.1128/AEM.71.12.8147-8156.2005.
132. S. Osman, Z. Peeters, M.T. La Duc, R. Mancinelli, P. Ehrenfreund, K. Venkateswaran, Effect of Shadowing on Survival of Bacteria under Conditions Simulating the Martian Atmosphere and UV Radiation, Appl. Environ. Microbiol. 74 (2008) 959–970. https://doi.org/10.1128/AEM.01973-07.
133. R. Moeller, M. Rohde, G. Reitz, Effects of ionizing radiation on the survival of bacterial spores in artificial martian regolith, Icarus 206 (2010) 783–786. https://doi.org/10.1016/j.icarus.2009.11.014.

 doi:10.20944/preprints202506.2121.v1

134. C. Mosca, L.J. Rothschild, A. Napoli, F. Ferré, M. Pietrosanto, C. Fagliarone, M. Baqué, E. Rabbow, P. Rettberg, D. Billi, Over-Expression of UV-Damage DNA Repair Genes and Ribonucleic Acid Persistence Contribute to the Resilience of Dried Biofilms of the Desert Cyanobacetrium Chroococcidiopsis Exposed to Mars-Like UV Flux and Long-Term Desiccation, Front. Microbiol. 10 (2019) 2312. https://doi.org/10.3389/fmicb.2019.02312.
135. M. Baqué, J.-P. de Vera, P. Rettberg, D. Billi, The BOSS and BIOMEX space experiments on the EXPOSE-R2 mission: Endurance of the desert cyanobacterium *Chroococcidiopsis* under simulated space vacuum, Martian atmosphere, UVC radiation and temperature extremes., Acta Astronaut. 91 (2013) 180–186. https://doi.org/10.1016/j.actaastro.2013.05.015.
136. D. Billi, C. Staibano, C. Verseux, C. Fagliarone, C. Mosca, M. Baqué, E. Rabbow, P. Rettberg, Dried Biofilms of Desert Strains of Chroococcidiopsis Survived Prolonged Exposure to Space and Mars-like Conditions in Low Earth Orbit, Astrobiology 19 (2019) 1008–1017. https://doi.org/10.1089/ast.2018.1900.
137. D. Billi, E.I. Friedmann, K.G. Hofer, M.G. Caiola, R. Ocampo-Friedmann, Ionizing-Radiation Resistance in the Desiccation-Tolerant CyanobacteriumChroococcidiopsis, Appl. Environ. Microbiol. 66 (2000) 1489–1492. https://doi.org/10.1128/AEM.66.4.1489-1492.2000.
138. T.L. Foster, L. Winans, R.C. Casey, L.E. Kirschner, Response of terrestrial microorganisms to a simulated Martian environment., Appl. Environ. Microbiol. 35 (1978) 730–737. https://www.ncbi.nlm.nih.gov/pmc/articles/PMC242914/ (accessed March 31, 2025).
139. B.J. Berry, D.G. Jenkins, A.C. Schuerger, Effects of Simulated Mars Conditions on the Survival and Growth of Escherichia coli and Serratia liquefaciens, Appl. Environ. Microbiol. 76 (2010) 2377–2386. https://doi.org/10.1128/AEM.02147-09.
140. T. Zaccaria, M.I. de Jonge, J. Domínguez-Andrés, M.G. Netea, K. Beblo-Vranesevic, P. Rettberg, Survival of Environment-Derived Opportunistic Bacterial Pathogens to Martian Conditions: Is There a Concern for Human Missions to Mars?, Astrobiology 24 (2024) 100–113. https://doi.org/10.1089/ast.2023.0057.
141. S.M. Montaño-Salazar, J. Lizarazo-Marriaga, P.F.B. Brandão, Isolation and Potential Biocementation of Calcite Precipitation Inducing Bacteria from Colombian Buildings, Curr. Microbiol. 75 (2018) 256–265. https://doi.org/10.1007/s00284-017-1373-0.
142. S. Shu, B. Yan, B. Ge, S. Li, H. Meng, Factors Affecting Soybean Crude Urease Extraction and Biocementation via Enzyme-Induced Carbonate Precipitation (EICP) for Soil Improvement, Energies 15 (2022) 5566. https://doi.org/10.3390/en15155566.
143. H. Rohy, M. Arab, W. Zeiada, M. Omar, A. Almajed, A. Tahmaz, One Phase Soil Bio-Cementation with EICP-Soil Mixing, in: 2019. https://doi.org/10.11159/icgre19.164.
144. J. Zehner, A. Røyne, P. Sikorski, A sample cell for the study of enzyme-induced carbonate precipitation at the grain-scale and its implications for biocementation, Sci. Rep. 11 (2021) 13675. https://doi.org/10.1038/s41598-021-92235-7.
145. T. Hoang, J. Alleman, B. Cetin, S.-G. Choi, Engineering Properties of Biocementation Coarse- and Fine-Grained Sand Catalyzed By Bacterial Cells and Bacterial Enzyme, J. Mater. Civ. Eng. 32 (2020) 04020030. https://doi.org/10.1061/(ASCE)MT.1943-5533.0003083.
146. J.S. Singh, P.C. Abhilash, H.B. Singh, R.P. Singh, D.P. Singh, Genetically engineered bacteria: an emerging tool for environmental remediation and future research perspectives, Gene 480 (2011) 1–9. https://doi.org/10.1016/j.gene.2011.03.001.
147. G. Pant, D. Garlapati, U. Agrawal, R.G. Prasuna, T. Mathimani, A. Pugazhendhi, Biological approaches practised using genetically engineered microbes for a sustainable environment: A review, J. Hazard. Mater. 405 (2021) 124631. https://doi.org/10.1016/j.jhazmat.2020.124631.
148. Committee on Space Research (COSPAR) » COSPAR Policy on Planetary Protection, COSPAR Website (n.d.). https://cosparhq.cnes.fr/cospar-policy-on-planetary-protection/ (accessed May 10, 2025).
149. M. Baqué, G. Scalzi, E. Rabbow, P. Rettberg, D. Billi, Biofilm and Planktonic Lifestyles Differently Support the Resistance of the Desert Cyanobacterium Chroococcidiopsis Under Space and Martian Simulations, Orig. Life Evol. Biospheres 43 (2013) 377–389. https://doi.org/10.1007/s11084-013-9341-6.

 doi:10.20944/preprints202506.2121.v1

150. Z. Fang, P. Knoll, S. McMahon, L. Qin, C.S. Cockell, Preservation of Microorganisms (Chroococcidiopsis sp. 029) in Salt Minerals under Low Atmospheric Pressure: Application to Life Detection on Mars, Planet. Sci. J. 5 (2024) 263. https://doi.org/10.3847/PSJ/ad8b1b.
151. J.A. Hoffman, M.H. Hecht, D. Rapp, J.J. Hartvigsen, J.G. SooHoo, A.M. Aboobaker, J.B. McClean, A.M. Liu, E.D. Hinterman, M. Nasr, S. Hariharan, K.J. Horn, F.E. Meyen, H. Okkels, P. Steen, S. Elangovan, C.R. Graves, P. Khopkar, M.B. Madsen, G.E. Voecks, P.H. Smith, T.L. Skafte, K.R. Araghi, D.J. Eisenman, Mars Oxygen ISRU Experiment (MOXIE)—Preparing for human Mars exploration, Sci. Adv. 8 (2022) eabp8636. https://doi.org/10.1126/sciadv.abp8636.
152. L.E. Fackrell, S. Humphrey, R. Loureiro, A.G. Palmer, J. Long-Fox, Overview and recommendations for research on plants and microbes in regolith-based agriculture, Npj Sustain. Agric. 2 (2024) 15. https://doi.org/10.1038/s44264-024-00013-5.
153. G.W.W. Wamelink, J.Y. Frissel, W.H.J. Krijnen, M.R. Verwoert, P.W. Goedhart, Can Plants Grow on Mars and the Moon: A Growth Experiment on Mars and Moon Soil Simulants, PLOS ONE 9 (2014) e103138. https://doi.org/10.1371/journal.pone.0103138.
154. M. RAMPINI, A. BACCHIEGA, Preliminary analysis of innovative inflatable habitats for Mars surface missions, (2021). https://www.politesi.polimi.it/handle/10589/173716 (accessed June 23, 2025).
155. D. Miles, ARTICLE: "Research Methods and Strategies Workshop: A Taxonomy of Research Gaps: Identifying and Defining the Seven Research Gaps," 1 (2017) 1.
156. S. Khoshtinat, C. Marano, Numerical Modeling of the pH Effect on the Calcium Carbonate Precipitation by Sporosarcina pasteurii, in: M. Kioumarsi, B. Shafei (Eds.), 1st Int. Conf. Net-Zero Built Environ., Springer Nature Switzerland, Cham, 2025: pp. 141–153. https://doi.org/10.1007/978-3-031-69626-8_13.
157. S. Khoshtinat, C. Marano, M. Kioumarsi, Computational modeling of biocementation by S. pasteurii: effect of initial pH, Discov. Mater. 5 (2025) 65. https://doi.org/10.1007/s43939-025-00241-7.